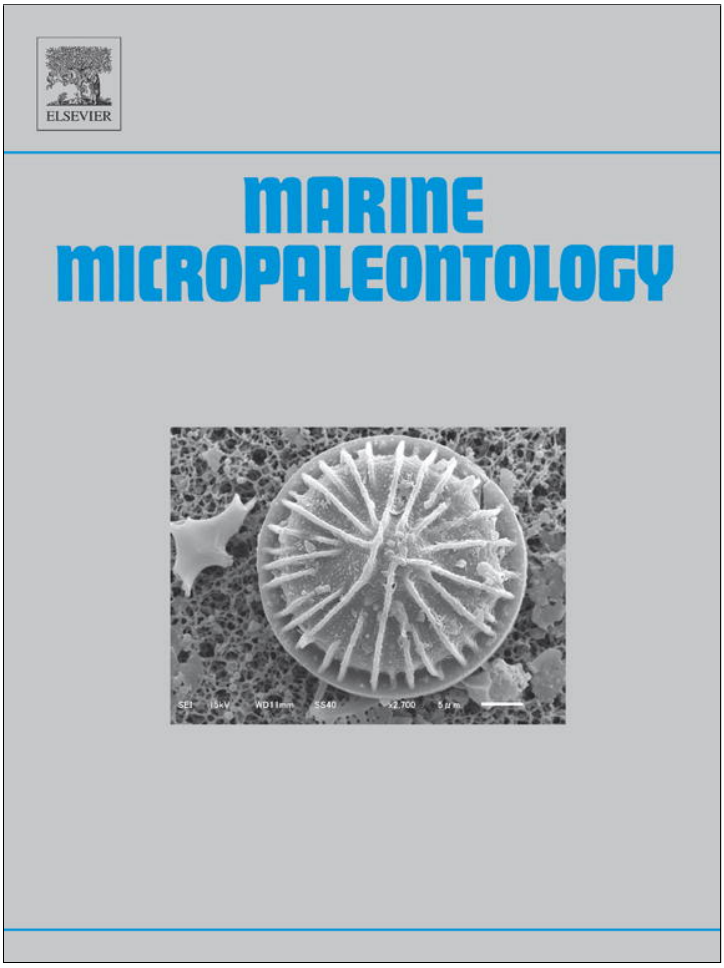
ELSEVIER
MARINE
MICROPALEONTOLOGY

Marine Micropaleontology 96-97 (2012) 13–28

Contents lists available at SciVerse ScienceDirect

Marine Micropaleontology

journal homepage: www.elsevier.com/locate/marmicro

Benthic and planktic community changes at the North Siberian margin in response to Atlantic water mass variability since last deglacial times

Ekaterina Taldenkova [a,*], Henning A. Bauch [b], Anna Stepanova [c], Yaroslav Ovsepyan [d], Irina Pogodina [e,1], Tatiana Klyuvitkina [a], Sergei Nikolaev [a]

[a] Geographical Faculty, Lomonosov Moscow State University, Moscow, Leninskie Gory, 1, 119991, Russia
[b] Mainz Academy for Science, Humanities and Literature, c/o GEOMAR, Wischhofstrasse, 1-3, 24148 Kiel, Germany
[c] Paleontological Institute RAS, Profsoyuznaya, 123, Moscow, 117997, Russia
[d] Geological Faculty, Lomonosov Moscow State University, Moscow, Leninskie Gory, 1, 119991, Russia
[e] Murmansk Marine Biological Institute, Vladimirskaya, 17, Murmansk, 183010, Russia

ARTICLE INFO

Article history:
Received 1 May 2011
Accepted 22 June 2012
Available online 6 July 2012

Keywords:
Atlantic-derived water
Laptev Sea
Planktic and benthic foraminifers
Ostracods
Deglaciation
Holocene

ABSTRACT

The eastward penetration of Atlantic-derived water (ADW) into the Eurasian Basin of the Arctic Ocean was investigated at the western Laptev Sea continental margin for the time since c. 17.6 ka. Using a high-resolution investigation of the lithology, geochemistry, planktic and benthic foraminifers, and ostracods on a sediment core from 270 m water depth major steps in the environmental evolution of the region are recognized. In general, ADW was continuously present in the study area. Between 17.6 and 15.4 ka ADW manifested itself through open-water polynyas and associated upwelling events. Comparison between the Laptev Sea and northern Svalbard shelf using *Cassidulina neoteretis* allows assuming an unmodified subsurface inflow of ADW within its northern branch between 15.4 and 13.2, which was strongest after 14.7-ka and in line with the overall climate amelioration. A local freshwater event at 13 ka followed by shelf flooding and the establishment of a freshened shelf water mass resulted in an off-shelf displacement of ADW from the studied site as suggested by the disappearance of *C. neoteretis* between 12 and 7 ka. As evidenced by an abundance peak in *Nonion labradoricum*, the sea-ice marginal zone was located at the site around 12–11 ka but then shifted northward during the early Holocene warming. Enhanced ADW inflow since 7 ka correlated with climate cooling and southward retreat of the seasonal drift-ice margin. The inflow of ADW during mid–late Holocene differed from deglacial times because of the combined influence of northern and eastern ADW branches.

1. Introduction

The recently observed changes in the Arctic which are commonly related to global warming are expressed not only by considerable shrinking of the summer sea-ice cover extent (Serreze et al., 2007; Comiso et al., 2008; Polyak et al., 2010), but also by intensification of Atlantic-derived water inflow together with the increasing temperature of Atlantic water layer (Schauer et al., 2004; Polyakov et al., 2005). Besides instrumental measurements the latter is also evidenced by unprecedented changes in the composition of planktic foraminifers from Fram Strait during the early 21st century compared to the previous 2 thousand years (Spielhagen et al., 2011). Knowledge about the extent and timing of past inflows of Atlantic-derived waters carrying heat and salt to the Arctic Ocean is crucial for reconstructing short and long-term climate changes. During interglacial epochs, inflows of Atlantic-derived waters resulted in generally milder climate conditions in the Arctic and reduced sea-ice cover with more open-water leads (Knies et al., 2000; Spielhagen et al., 2004; Polyak et al., 2010). There is evidence that the subsurface inflows of these waters along Eurasian continental margin could be quite intense during both deglacial and glacial times (Knies et al., 1999; Bauch et al., 2001a; Nørgaard-Pedersen et al., 2003; Kristoffersen et al., 2004; Wollenburg et al., 2004; Rasmussen et al., 2007). Different patterns of Atlantic water inflows to subarctic Nordic seas and adjacent Eurasian Arctic periphery in relation to the extent and disintegration of the Barents-Kara ice sheet and water mass changes during lateglacial to Holocene times are fairly well reconstructed (Polyak and Mikhailov, 1996; Polyak et al., 1997; Hald et al., 1999; Bauch et al., 2001a; Duplessy et al., 2001; Hald et al., 2001; Lubinski et al., 2001; Ivanova et al., 2002; Koç et al., 2002; Hald et al., 2003, 2004; Duplessy et al., 2005; Ślubowska et al., 2005; Ebbesen et al., 2007; Hald et al., 2007; Rasmussen et al., 2007; Ślubowska-Woldengen et al., 2007, 2008; Aagard-Sørensen et al., 2010; Chistyakova et al., 2010; Risebrobakken et al., 2010). Contrary to this, sediment records from Siberian Arctic

* Corresponding author. Tel.: +7 495 9391608; fax: +7 495 9328836.
E-mail addresses: etaldenkova@mail.ru (E. Taldenkova), hbauch@geomar.de (H.A. Bauch), a.yu.stepanova@gmail.com (A. Stepanova), yaovsepyan@yandex.ru (Y. Ovsepyan), t.klyuvitkina@mail.ru (T. Klyuvitkina), cdnik@rambler.ru (S. Nikolaev).
[1] Passed away on 12.05.2011.

0377-8398/$ – see front matter © 2012 Elsevier B.V. All rights reserved.
doi:10.1016/j.marmicro.2012.06.007

margins further eastward are considerably less studied primarily due to the lack of cores with reliable chronologies.

One of the better records with sufficient time resolution and radiocarbon chronology is a core from the upper slope of the western Laptev Sea continental margin (Fig. 1). The core dates back to c. 17.6 cal.ka and represents so far the longest radiocarbon-controlled record of postglacial and Holocene events in the region. As shown previously, the core holds evidence of iceberg-rafting events and meltwater inputs

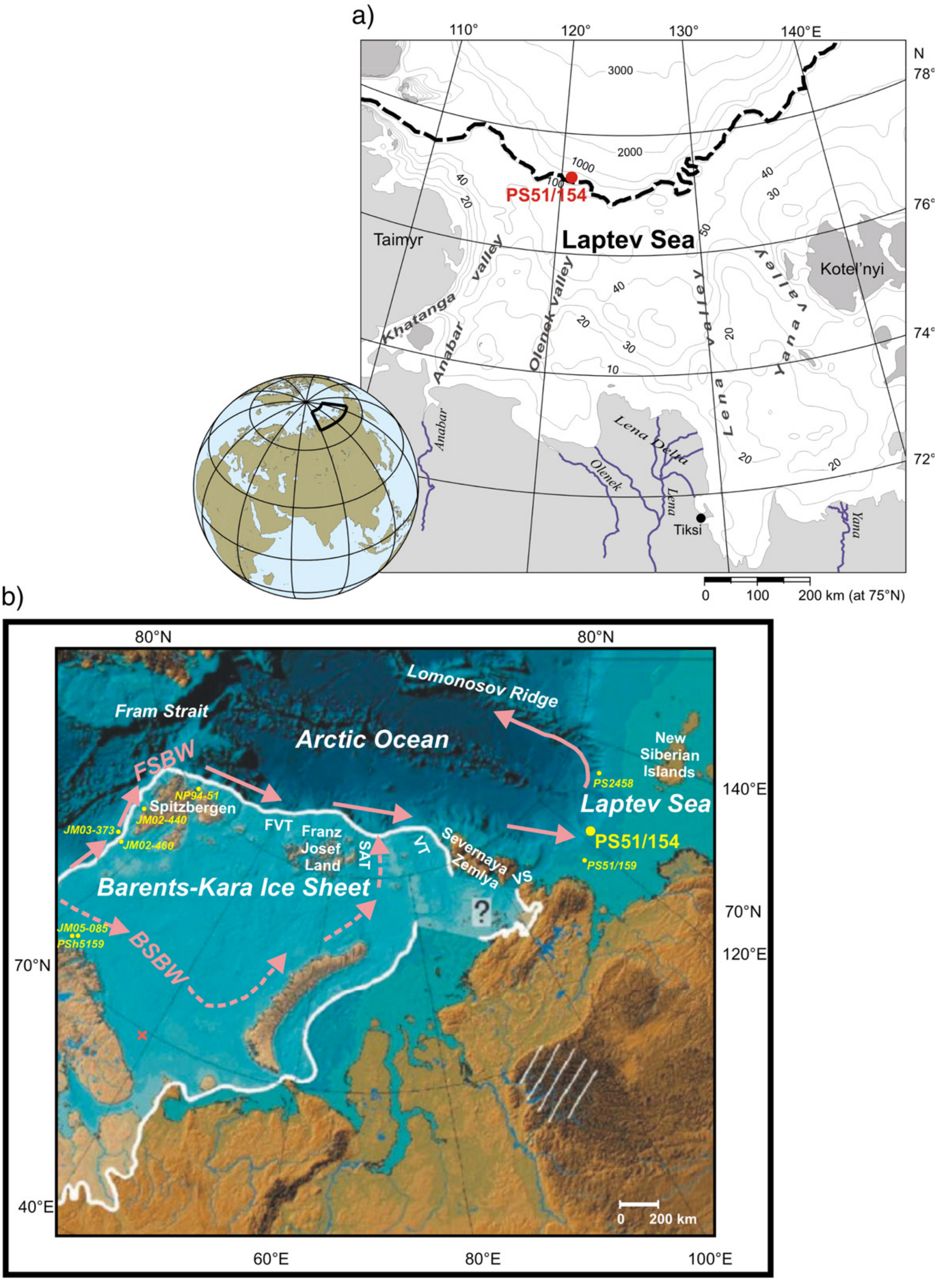

Fig. 1. a. Location of core PS51/154 in the Laptev Sea. Dashed line along the 100 m isobath shows the approximate position of the shoreline during the last glacial time. Major river paleovalleys are indicated. b. Extent of the Barents–Kara Ice Sheet during the LGM (after Svendsen et al., 2004). Arrows correspond to the main pathways of Atlantic-derived water masses in the Arctic; FSBW — Fram Strait Branch Water, BSBW — Barents Sea Branch Water. Other cores mentioned in the text are shown. FVT — Franz Victoria Trough, SAT — St. Anna Trough, VT — Voronin Trough, VS — Vilkitskii Strait.

as well as the regional manifestations of Atlantic-derived water (ADW) masses influence (Taldenkova et al., 2010). The latter was already indicated by the presence of typical, Atlantic-water indicative microfossils, e.g., benthic foraminifer *Cassidulina neoteretis* and subpolar planktic foraminifers. However, in order to gain a better understanding of the interactions between ADW and climatically-controlled freshwater input, variability in sea-ice cover extent and productivity changes we now combine data on lithology, geochemistry and microfossils. Especially important for interpretation are benthic foraminifers, as this group has proven itself to be a reliable indicator of environmental change in Arctic marginal seas (Hald et al., 1994; Korsun et al., 1994; Steinsund et al., 1994; Wollenburg and Mackensen, 1998; Polyak et al., 2002; Ślubowska-Woldengen et al., 2008). In this study, we analyze high-resolution continuous records of benthic and planktic foraminifers, ostracods and lithology from the Laptev Sea continental margin and correlate the observed paleoceanographic events with those recorded farther west, i.e., along the flowpath of ADW in the Arctic Ocean.

2. Modern setting

The inflow of the warm and saline Atlantic water to the Arctic Ocean and its marginal seas, which is driven by thermohaline and estuarine forcing as well as winds, has a profound effect on the arctic environment (ACIA, 2005). Atlantic waters enter the Arctic Ocean via two main branches (Rudels et al., 2004; Saloranta and Haugan, 2004; Carmack et al., 2006) (Fig. 1). The Fram Strait Branch Water (FSBW) flows north of Svalbard with the West Spitsbergen current. The Barents Sea Branch Water (BSBW) is formed from interactions between the Atlantic Water flowing into the southwestern Barents Sea and local fresher and colder Barents and Kara shelf waters. Besides the difference in temperature and salinity characteristics, these Atlantic-derived water masses have specific phytodetrital deposition and nutrient composition that are essential for benthic species occurring within or underneath these water masses (Lubinski et al., 2001; Wollenburg et al., 2004). After entering the Arctic Ocean ADW submerges beneath the fresher and colder polar water and flows eastward in the depths of 150–800 m along the continental slope.

In the Laptev Sea, the warm core of ADW (temperature 0.5–1.5 °C, salinity 34.7–34.9) is usually located in 150–350 m water depth range (Dmitrenko et al., 2008). It is subject to seasonal on/offshore movements probably related to seasonal wind variations (Dmitrenko et al., 2006). Interactions between shelf and slope water masses could be also induced by offshore winds producing reversed bottom water currents that can periodically penetrate the outer and middle shelf (Dmitrenko et al., 2001, 2010). Another important mechanism of shelf-slope interactions in the western Laptev Sea is dense water cascading in its north-western part. It results from ice freeze-up and brine ejection in coastal polynyas along the steep slope. These waters penetrate downslope and contribute to cooling and freshening of ADW (Ivanov and Golovin, 2007).

The Laptev Sea shelf is contoured by the 80–100 meter lines (Fig. 1). It is cut by several paleoriver valleys formed in the Pleistocene during times of sea-level lowstands (Bauch et al., 1999, 2001b; Bauch and Kassens, 2005; Darby et al., 2006). The shelf hydrography is characterized by the interaction of freshwater input from large Siberian rivers, primarily the Lena River, cold brines produced from sea-ice formation, and meltwater input during summer sea-ice melting. In winter, the entire area is ice-covered besides wind-induced narrow open-water leads, so-called polynyas which separate the fast from the drift ice. Although the Laptev Sea becomes largely ice-free during the short summer season, changeable wind patterns can make a major difference on an interannual basis. For instance, in the western Laptev Sea a sea ice massif may exist perennially, often blocking Vilkitskii Strait thereby occupying between 25 and 75% of the western Laptev Sea in September (Karklin and Karelin, 2009).

3. Material and methods

Core PS51/154-11 was obtained from the upper continental slope of the western Laptev Sea (77°15,56 N, 120°36,59E, water depth 270 m) during TRANSDRIFT V expedition aboard RV Polarstern in 1998 (Fig. 1).

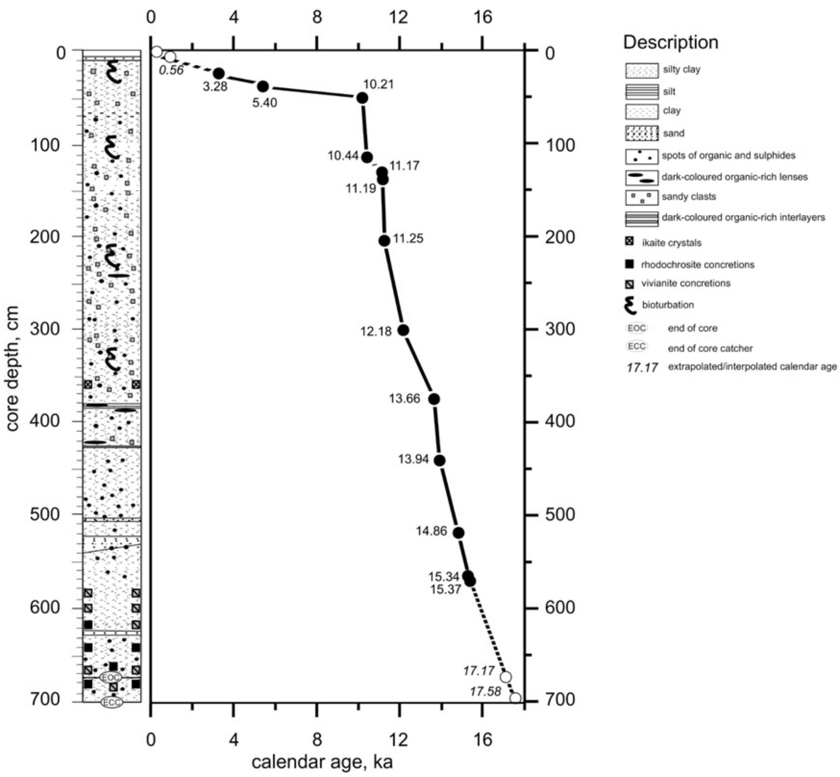

Fig. 2. Lithofacies log and age-depth relationship of core PS51/154. Details of calendar age calculation are given in Table 1.

Table 1
Radiocarbon (AMS) dates and calibrated age (Bauch et al., 2001b; Taldenkova et al., 2010).

Lab #	Depth, cm	Material	Radiocarbon age	Calendar age calculated with calibration version Fairbanks 0107		
				Mean	1 std dev	ΔR
KIA-27682	25	Foraminifers/*Yoldiella* sp.	3425 ± 30	3279[a]	46	370
KIA-6919	31	*Yoldiella intermedia*	1540 ± 45	1079	61	370
KIA-32810	39	Foraminifers	5040 ± 50	5398[a]	73	370
KIA-32811	39	Bivalves/gastropod	1800 ± 35	1322	24	370
KIA-27683	51	Foraminifers/ostracods/*Yoldiella* sp.	9570 ± 60	10347	93	370
KIA-32812	73	Foraminifers	9410 ± 70	10208[b]	55	370
KIA-32813	73	*Yoldiella lenticula*	9605 ± 45	10401	84	370
KIA-27684	85	Foraminifers/*Portlandia arctica*	9505 ± 50	10265	49	370
KIA-32814	115	*Yoldiella lenticula*	9630 ± 50	10442[a]	85	370
KIA-32815	131	*Nucula tenuis*	10085 ± 45	11165[a]	51	370
KIA-6920	138	*Macoma calcarea*	10120 ± 55	11187[a]	44	370
KIA-6921	204	*Nucula tenuis*	10235 ± 45	11250[a]	33	370
KIA-6922	300	*Yoldiella intermedia*	10725 ± 50	12175[a]	108	370
KIA-6923	375	*Yoldiella lenticula*	12180 ± 60	13661[a]	65	370
KIA-6924	440	*Yoldiella intermedia*	12525 ± 55	13941[a]	73	370
KIA-6925	518	Foraminifers/*Portlandia arctica*	13120 ± 60	14856[a]	105	370
KIA-9976	567	Foraminifers	13540 ± 90	15338[a]	145	370
KIA-9977	569	Foraminifers	13570 ± 110	15372[a]	162	370

[a] Datings taken for age model calculation.
[b] Dating assigned for 51 cm core depth (see text for explanation).

It is a gravity kasten core with a core recovery of 675 cm (700 cm including core catcher; Fig. 2). The upper 6 cm was lost during coring. Hereafter, for simplicity the core will be named PS51/154.

The chronology of the core is based on radiocarbon ages from marine biogenic calcite (single bivalve shells and/or mixed foraminifers) determined by means of accelerator mass spectrometry (AMS) at the Leibniz Laboratory in Kiel (Table 1).

The whole sediment sequence was sampled continuously in 2 cm thick slices. Samples were freeze-dried and subsequently washed over a 63-μm-mesh size sieve to determine the proportion of coarse fraction. Lithic grains were counted in the fraction > 500 μm.

Samples for geochemical analysis were taken at 5 cm intervals in the upper 150 cm, and at 10 cm intervals in the remainder. Freeze-dried and milled bulk samples of sediments (1 g) were taken to determine the contents of total organic carbon (TOC), total carbon (TC), and total nitrogen (TN). Measurements were carried out with a carbon–nitrogen–sulfur analyzer (Elementar Vario EL III). All samples were run in duplicate of which the average was used. C/N ratios were calculated as total organic carbon/total nitrogen ratios based on weight percentages. The carbonate content is calculated as $CaCO_3$ (%) = (TC − TOC) ∗ 8.333, where TC — total carbon (%), TOC — total organic carbon (%). Mass accumulation rates of TOC are calculated using linear sedimentation rates (LSR) for certain intervals between datings and assuming sediment density to be 1 g/cm^3 (Figs. 2, 3).

All microfossils were picked from washed samples (> 63 μm fraction) without splitting the sediment. The only exception was the basal sample of the core, which contained extremely abundant planktic foraminifers in the fraction 63–125 μm. From this sample all planktic foraminifers were picked from the > 125 μm fraction, whereas the fraction 63–125 μm was split 4 times to obtain 450 specimens for counting. The total abundance of microfossils is expressed as specimens per 100 g dry bulk weight (Figs. 4, 7). Relative proportions of species and ecological groups of benthic foraminifers were estimated for samples which contained more than 100 specimens (Figs. 5, 9). Because of their scarcity, no relative abundance plots were produced for planktic foraminifers and ostracods, and species/ecological groups occurrence is shown as specimens per 100 g dry bulk weight (Figs. 6–9). The taxonomic list of all species of foraminifers and ostracods identified in core PS51/154 is given as Supplementary online information.

The interpretation of the various microfossil assemblages with regard to ecological groups and index-species is based on published and/or our own observations using their modern distribution in surface sediments. For benthic foraminifers, we use the classification of Polyak et al. (2002) who distinguished three ecological groups in

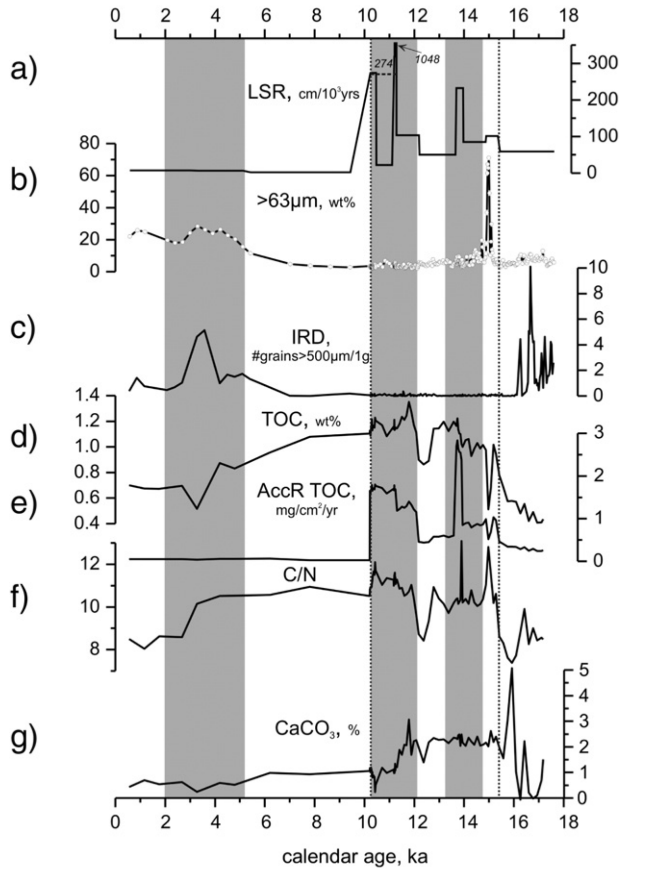

Fig. 3. Lithological and geochemical characteristics of core PS51/154: a) linear sedimentation rates (LSR); b) weight percentage of sediment fraction > 63 μm; c) ice- and iceberg-rafted debris (IRD), lithic grains > 500 μm; d) total organic carbon content; e) mass accumulation rates of the total organic carbon; f) C/N ratio; g) $CaCO_3$ content. Vertical dotted lines show the boundaries of sediment units. Shading corresponds to the time intervals of prominent changes in the composition of benthic foraminifers.

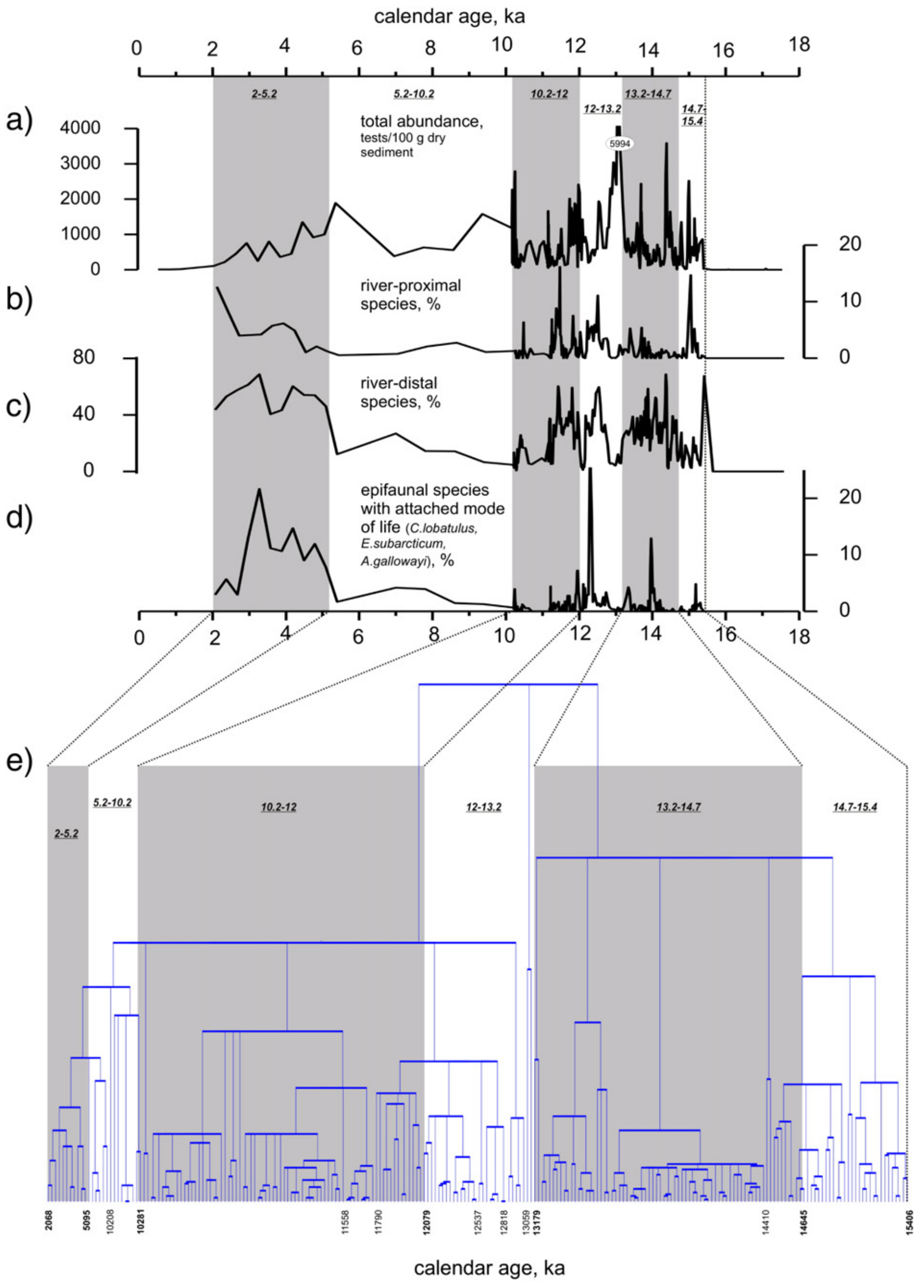

Fig. 4. Distribution of benthic foraminifers in core PS51/154: a) total abundance; b) river-proximal species; c) river-distal species; d) epifaunal species with attached mode of life; e) cluster analysis dendrogram of 234 core samples based on total abundance of benthic foraminifers and relative abundance of 11 major species and 4 ecological groups. Shading corresponds to the time intervals of prominent changes in the composition of benthic foraminifers.

river-affected Arctic environments: river-proximal, river-intermediate, and river-distal. In the studied core (Fig. 4), the river-proximal group consists of four species — *Haynesina orbiculare*, *Elphidium incertum*, *Elphidium bartletti*, and *Buccella frigida*. The river-distal group is more abundant and includes *Astrononion gallowayi*, *Melonis barleeanus*, *Cibicides lobatulus*, *Islandiella norcrossi/helenae*, *Islandiella islandica* and *C. neoteretis*. Three species, *Cibicides lobatulus*, *Astrononion gallowayi*, and *Elphidium subarcticum*, comprise a group of epifaunal species with an attached mode of life, that is, they settle on coarse lithic grains (Fig. 4). In the assemblages we recognized a number of time intervals with prominent changes in the composition of the benthic foraminifers (shadings in Figs. 3–9). In order to further support the visual subdivision of the benthic foraminiferal record into time intervals we therefore employed a cluster analysis. The data of total abundance and percentages of 11 major species and 4 ecological groups from a total of 234 benthic foraminiferal samples (those with > 100 specimens per sample) were entered into the PAST software package (Hammer et al., 2001) to produce a cluster dendrogram. We apply unweighted pair-group average (UPGMA) using basic Euclidean distance for stratigraphically constrained R-mode clustering.

Planktic foraminifers are mainly represented by the polar species *Neogloboquadrina pachyderma* sin. which is typical for the Arctic. In addition, we also observe a diverse subpolar assemblage, but at very discrete intervals only (Fig. 6).

Ostracods were shown to be good indicators of salinity changes on the Laptev Sea shelf and slope (Stepanova et al., 2003, 2007). They are represented by several ecological groups ranging from freshwater to relatively deep-water marine ones (Fig. 7). Among the latter, a group of shelf-upper slope North Atlantic species (Whatley and Masson, 1979; Whatley et al., 1998) is distinguished,

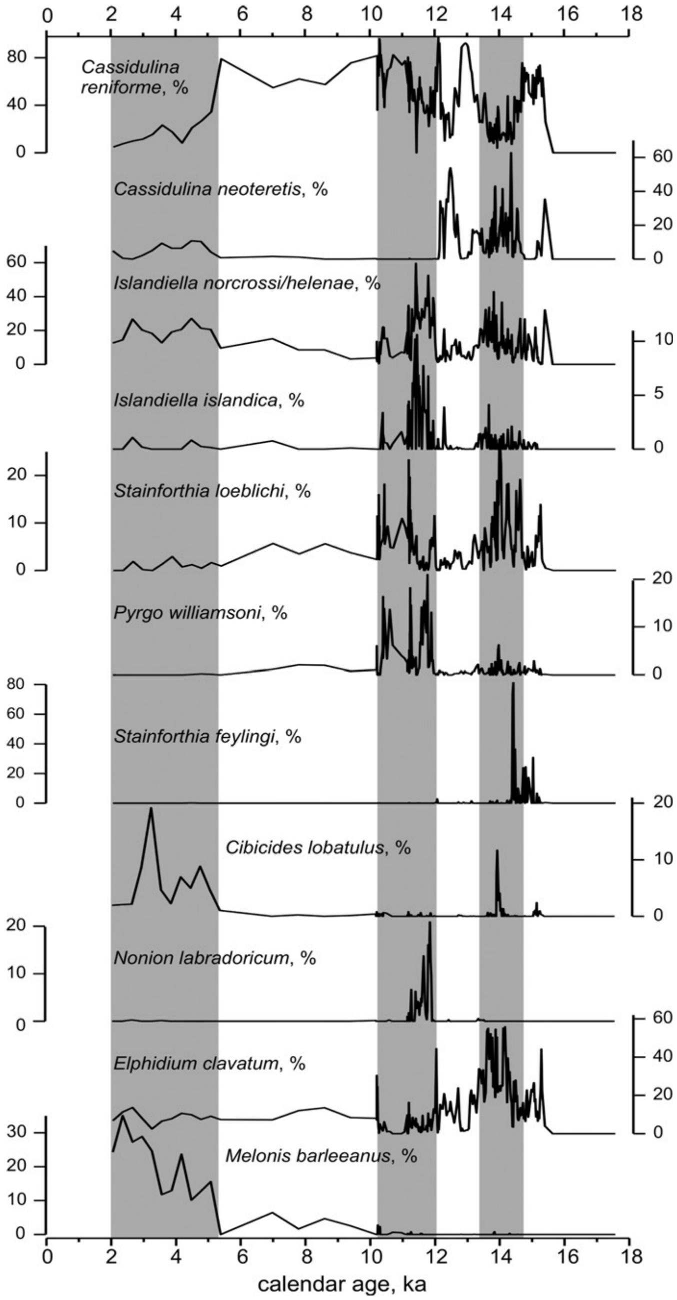

Fig. 5. Distribution of benthic foraminifers in core PS51/154: relative abundances of major species. Shading corresponds to the time intervals of prominent changes in the composition of benthic foraminifers.

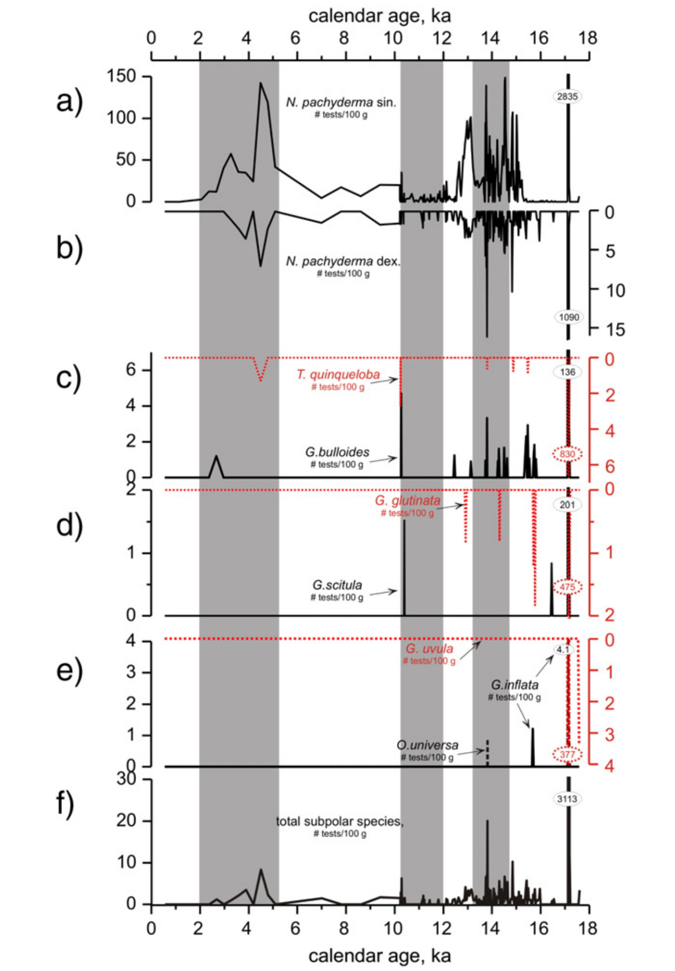

Fig. 6. Distribution of planktic foraminifers in core PS51/154: a–e) abundances of different species; f) total abundance of subpolar planktic foraminifers. Mind reversed scales for *N. pachyderma* dex., *T. quinqueloba*, *G. glutinata*, *G. uvula*. Figures in circles correspond to the out-of-scale-high abundance at c. 17.2 ka. Shading corresponds to the time intervals of prominent changes in the composition of benthic foraminifers.

which includes *Cytheropteron arcuatum*, *Cytheropteron biconvexa*, *Cytheropteron inflatum*, *Cytheropteron laptevensis*, *Cytheropteron occultum*, *Cytheropteron paralatissimum*, *Cytheropteron perlaria*, *Cytheropteron porterae*, *Cytheropteron pseudomontrosiense*, *Cytheropteron tumefactum*, *Bythocythere constricta*, *Pseudocythere caudata* (Fig. 8; Stepanova et al., 2003, 2004; Stepanova, 2006; Stepanova et al., 2007; Cronin et al., 2010). These ostracods with North Atlantic affinities are regarded, together with planktic foraminifers (especially subpolar species) and the benthic foraminifer species *C. neoteretis*, as the main indicators of ADW in the Laptev Sea region.

The original data on dinoflagellate cysts from core PS51/154 were published previously (Klyuvitkina, 2007; Klyuvitkina et al., 2009). Here we now present the distribution of AH-ratio and relative abundance of the species *Operculodinium centrocarpum* (Fig. 9). The AH-ratio, which expresses the proportion between autotrophic and heterotrophic dinoflagellate species, gives evidence for paleoproductivity, duration of sea-ice cover season, and the influence of ADW in the Arctic seas (Bujak, 1984; Mudie, 1992; Mudie and Rochon, 2001; Klyuvitkina and Bauch, 2006). Although *O. centrocarpum* occurs in the surface sediments of polar regions, its maximum abundance is observed in temperate latitudes of the eastern Nordic seas (Mudie, 1992; Rochon et al., 1999). In the Arctic, this species can therefore be regarded as an indicator of ADW inflow (Matthiessen et al., 2005; Klyuvitkina and Bauch, 2006).

4. Results

4.1. Core chronology and sedimentation rates

The core chronology is constrained by eighteen AMS^{14}C dates (Table 1, Fig. 2). For converting the AMS^{14}C dates to calendar years B.P. (ka) using the Fairbanks 0107 program (Fairbanks et al., 2005), a reservoir age of 370 years, as the determined for the modern Laptev Sea (Bauch et al., 2001b), was applied. All dates mentioned in the text are in *calendar* years.

For age model calculations we excluded the two reversal datings from 31 and 39 cm depth obtained on molluscs (Table 1). These datings are most likely the result of burrowing of bivalves into the sediment sequence accumulated under low sedimentation rates (Figs. 2, 3). The whole sediment section between 51 and 115 cm is more heavily

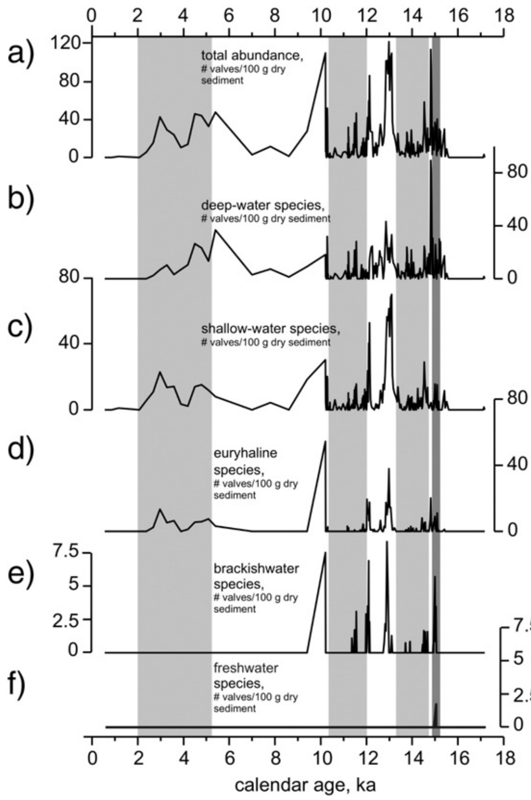

Fig. 7. Distribution of ostracods in core PS51/154: a) total abundance; b–f) abundances of different ecological groups. Shading corresponds to the time intervals of prominent changes in the composition of benthic foraminifers. Dark gray shading marks the prominent slide event at about 15 ka.

bioturbated and shows, within errors, practically a similar age (Table 1). Because of that we only used the youngest and the oldest datings for the age model, and the dating obtained on foraminifers from 73 cm depth was assigned to 51 cm core depth. Ages between the 13 dated fixpoints were estimated by linear interpolation and assuming a modern age for the sediment surface. The extrapolated age of the sediment record base (core catcher (CC) base) is 17.6 ka, and that of the core itself 17.2 ka (Table 1, Fig. 2). With the upper 6 cm removed during coring, the actual core top gave an interpolated age of 0.6 ka (Fig. 2).

Regardless of the age uncertainties associated with the upper part of the core, linear sedimentation rates (LSR) were generally high prior to 10 ka, with peaks at around 14, 11 and 10 ka (Fig. 3). Because the peak at 11 ka occurs together with signs of enhanced bioturbation, which would rather indicate reduced LSR (see above paragraph), we calculated a mean LSR for the interval 51–115 cm (274 cm/kyrs). It seems more reasonable to conclude that there were two major periods of elevated sedimentation rates, about 14–13.5 ka and 11.2–10.2 ka. The sharply reduced LSR down about just 5 cm/kyrs after 10.2 ka, i.e. is the result of the reorganization of the depositional environment after the onset of extensive Laptev Sea shelf flooding (Bauch et al., 2001b).

4.2. Lithology, organic carbon and carbonate contents

The 700 cm-thick sediment sequence of the core and core catcher is represented by grayish clayey silt and silty clay with sandy lenses in the lower half of the section and with signs of bioturbation in the upper one (Fig. 2). Lithologically, the core is subdivided into three sediment units: the lower unit of the core (17.6–15.4 ka) is impoverished in fossils, but enriched in mica flakes, ice-rafted debris (IRD), and authigenic concretions of vivianite ($Fe_3[PO_4]x8H_2O$) and rhodochrosite ($MnCO_3$) (Figs. 2, 3). All these characteristics indicate periods of active iceberg-rafting truncated by intervals of freshwater-induced stratification and heavier sea ice-cover (Taldenkova et al., 2010). The middle unit (15.4–10.2 ka) is highly fossilferous, contains abundant plant debris, and is almost devoid of IRD. At the base of this unit a major sand–fraction spike occurs which probably relates to a sliding event because of the size uniformity of the particles (Figs. 2, 3) including valves of brackishwater and freshwater ostracods (Fig. 7). The fossiliferous upper sediment unit (10.2–0.6 ka) accumulated under very low sedimentation rates and is distinguished by high average percentage of the >63 μm fraction and high IRD concentrations both evidencing a re-establishment of iceberg-rafting in the region (Taldenkova et al., 2010).

Organic carbon content of the bottom sediments is generally dependent upon primary productivity, terrestrial input, granulometric composition, and preservation during sedimentation and early diagenesis, i.e., sedimentation rates and redox conditions (Romankevich and Vetrov, 2001; Murdmaa et al., 2004). In core PS51/154 TOC content varies from 0.4% in the oldest lateglacial sediments to highest values of 1.2–1.3% found at 12–11 ka (Fig. 3), the latter being comparable with the modern values of 1.0–1.5% (Stein, 2008). TOC content also correlates with the granulometric composition of sediments as exemplified by the drop in TOC within the sand layer at 15 ka. Relatively low values are also found in the lower (>15.4 ka) and upper (<10.2 ka) sediment units, partly associated with a coarser sediment composition. Another reason for low TOC levels is a reduction in sedimentation rates, especially in the Holocene interval. TOC accumulation rates became sharply reduced at 10.2 ka following the shelf flooding and southward migration of sediment depocenters and the coastline (Bauch et al., 2001b). Organic matter in the modern Laptev Sea sediments has been shown to have a dominant contribution of terrestrial component delivered by rivers and coastal erosion (Boucsein and Stein, 2000; Mueller-Lupp et al., 2000; Stein and Fahl, 2000; Stein, 2008). Therefore, the highest TOC concentrations recorded in the middle sediment unit (14–10.2 ka) are most likely a manifestation of the growing fluvial influence upon the site. The drop in TOC content in the middle of this sediment unit, between 13 and 12 ka, is related to the decrease in sedimentation rates and probably points to a reduction in river runoff influence and activity of coastal abrasion due to heavier sea-ice cover. The simultaneous reduction of C/N ratios is more difficult to explain. The C/N ratio has been used to distinguish between terrestrial organic matter, which shows ratios >15, and marine organic matter with ratios <10 (Knies et al., 1999; Vogt et al., 2001) or even <7 (Stein, 2008). As seen in our record, terrestrial organic matter prevailed throughout the section. It was only after about 3 ka, when C/N ratios decrease to 8–9 and more marine matter began to accumulate, that the modern-like marine environment became established. In this context, similar C/N values found during 13–12 ka might evidence either increased phytoplankton productivity or a contribution of inorganic nitrogen (Stein, 2008). The latter assumption seems likely since an increased productivity is exemplified by the increase in TOC and a decrease in C/N as observed between 13.7 and 13 ka and, especially, around 12–11 ka (Fig. 3).

The very low C/N ratios in the lower sediment unit (>15.4 ka) are likely related to diagenetic alterations. In this part of the section, authigenic concretions of vivianite occur, and the lowermost C/N values of 8 precisely correspond to the peak in vivanite which is observed after the IRD input ceased (Fig. 3; Taldenkova et al., 2010). Also, the spikes in $CaCO_3$ content in the lower sediment unit, which is almost devoid of any calcareous microfossils, seem to be somehow related to the occurrence of concretions. Highest $CaCO_3$ contents of about 5% correlate with a peak in vivianite at c. 16.2–15.8 ka, whereas the 0% content of $CaCO_3$ corresponds to the major concretion-formation event at about 17.2–16.8 ka, when both vivianite and rhodochrosite co-occur (Taldenkova et al., 2010). In the more fossiliferous part of the core, $CaCO_3$ content shows a positive correlation with the total abundance of calcareous microfossils (Figs. 3, 4, 7).

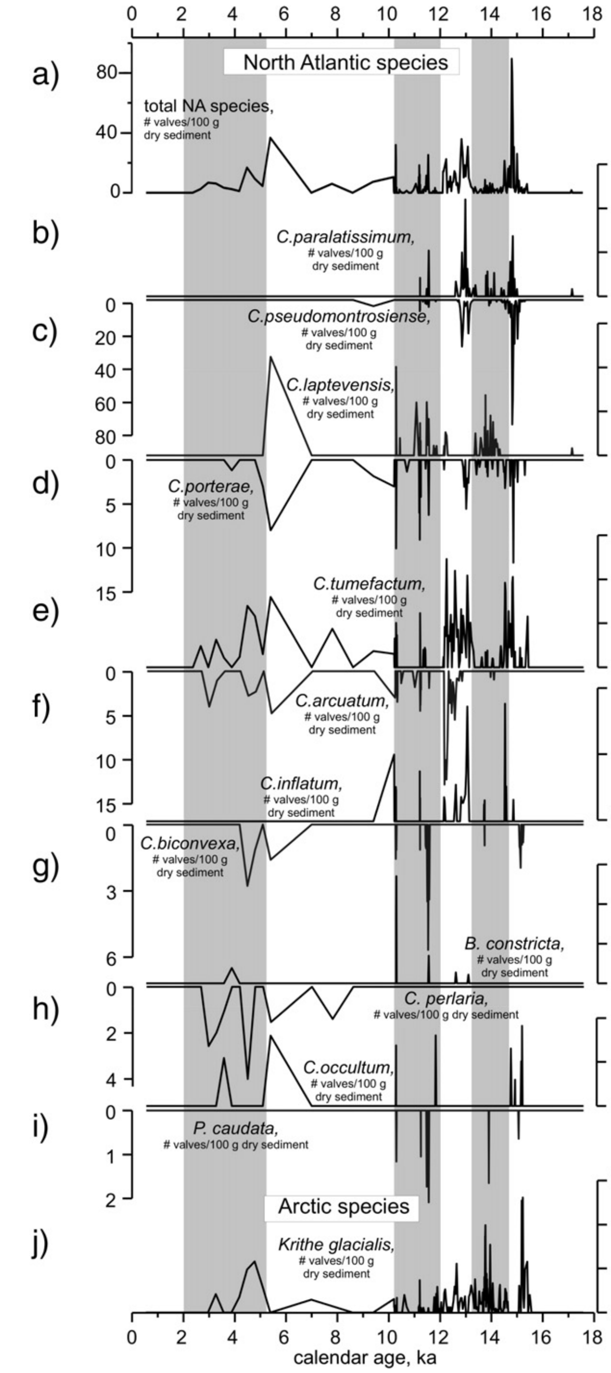

Fig. 8. Distribution of ostracods in core PS51/154: a) total abundance of North Atlantic species; b–j) abundances of different species. Mind reversed scales for *C. pseudomontrosiense*, *C. porterae*, *C. arcuatum*, *C. biconvexa*, *C. perlaria*, *P. caudata*. Shading corresponds to the time intervals of prominent changes in the composition of benthic foraminifers.

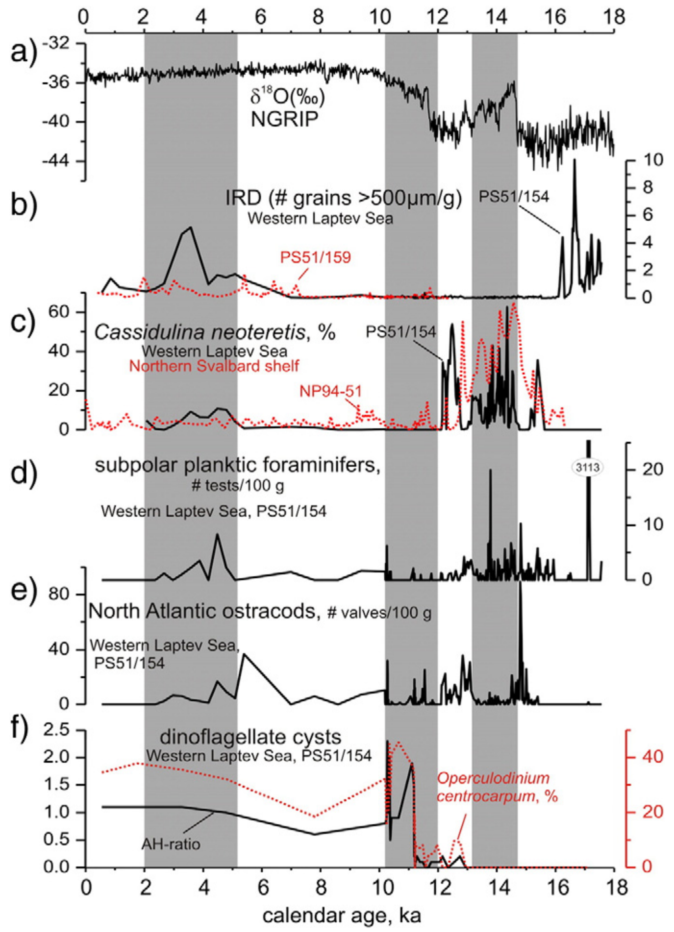

Fig. 9. Overregional comparison of the western Laptev Sea records with North Atlantic and western Arctic data: a) NGRIP oxygen isotope record (http://www.iceandclimate.nbi.ku.dk/data/); b) IRD record from the western Laptev Sea upper continental slope (PS51/154) and outer shelf (PS51/159); c) record of *Cassidulina neoteretis* percentage in the western Laptev Sea upper continental slope (PS51/154) and northern Svalbard shelf (NP94-51; Ślubowska et al., 2005; Ślubowska-Woldengen et al., 2008); d–f) records from the western Laptev Sea upper continental slope (PS51/154): d) total abundance of subpolar planktic foraminifers; e) total abundance of North Atlantic ostracods; f) dinocyst AH-ratio and relative abundance of *Operculodinium centrocarpum*. Shading corresponds to the time intervals of prominent changes in the composition of benthic foraminifers.

4.3. Benthic foraminifers

Calcareous benthic foraminifers are the major component of microfossil assemblages in core PS51/154 (Figs. 4, 5). They occur throughout the sediment sequence besides the lower sediment unit (>15.4 ka), where they are almost absent due to the prevalence of anaerobic bottom water conditions as indicated by authigenic concretions (Taldenkova et al., 2010). The co-occurrence of the perfectly preserved tests of rare planktic foraminifers (Fig. 6) eliminates calcite dissolution as the possible explanation for the absence of benthics. However, there are two short intervals within this unit where single benthic foraminifers do occur, at c. 17.2 and 16.2 ka, time-coeval with IRD peaks (Taldenkova et al., 2010). The assemblage is comprised of the species *Cassidulina reniforme*, *C. neoteretis*, *I. norcrossi*/*helenae*, *Elphidium clavatum*, *Nonion labradoricum*, *Pyrgo williamsoni*, *B. frigida*, *Quinqueloculina* spp. In sediments younger than 15.4 ka preservation of tests is good, especially between 15.4 and 12 ka. Only between 12 and 10.2 ka are there some tests with fragmentation and traces of corrosion. Preservation of tests is generally good in the Holocene section except the uppermost 15 cm (<2 ka), where calcareous foraminifers are sparse and replaced by agglutinated forms.

Time interval 15.4–14.7 ka is characterized by the predominance of *C. reniforme* (60–70%), a typical arctic cold-water species preferring salinities above 30, but able to tolerate slightly more freshened environments with reduced food supply (Korsun et al., 1994; Steinsund et al., 1994; Polyak et al., 2002). High percentages of opportunistic species *E. clavatum* and cold-water *Stainforthia loeblichi* indicate heavy seasonal sea-ice conditions (Hald et al., 1994; Ślubowska et al., 2005). An opportunistic species *Stainforthia feylingi* which reaches up to 20–30% gives evidence for unstable environment with periodically low oxygen conditions at the sea floor (Knudsen and Seidenkrantz, 1994; Knudsen et al., 2008). Arctic species *I. norcrossi*/*helenae*, *I. islandica*, and *Cibicides lobatulus* are characteristic of cold and saline water environment (Steinsund et al., 1994; Polyak et al., 2002). Rather remarkable is the high abundance of *C. neoteretis* (averaging 15–20%) as this would manifest a continuous presence of chilled and saline ADW at the site. This is because the occurrence of *C. neoteretis* at the Arctic continental margins is clearly restricted to the areas influenced by modified Atlantic waters, and seems to avoid regions with admixture of freshened shelf waters (Steinsund et al., 1994; Wollenburg and Mackensen, 1998; Osterman et al., 1999; Lubinski et al., 2001; Wollenburg et al., 2004). This species has also been found to be related to areas of brine release from sea ice freezing at the surface (Knudsen et al., 2008), and to be common in seasonally ice-free conditions with high seasonal productivity (Rasmussen et al., 2007). Food preferences of *C. neoteretis*, probably phytodetritus or associated bacteria, reflect an association with FSBW with relatively high phytodetrital deposition, temperature and salinity (Wollenburg and Mackensen, 1998; Lubinski et al., 2001).

Time interval 14.7–13.2 ka is distinguished by the highest relative abundance of *E. clavatum* (40–60%) in the core pointing to more freshened and turbid waters (Hald et al., 1994). Compared to *C. reniforme*, a predominance of *E. clavatum* suggests more stratified conditions (Duplessy et al., 2001). The highest percentages of *S. loeblichi* (15–25%) confirm this interpretation and give evidence for strong seasonality as this infaunal opportunistic species takes advantage of pulses of high seasonal productivity (Polyak et al., 2002). Like in the case with the previous time interval, high percentages of these species point to seasonally heavy sea-ice conditions. The tendency towards enhancement of seasonal productivity is corroborated by increasing percentages of *Islandiella* spp. and *P. williamsoni*. An exceptionally high spike of up to 80% of *S. feylingi* at 14.4 ka likely indicates reduced ventilation resulting from enhanced productivity (Knudsen et al., 2008). Subsurface ADW inflow was strong and constant as seen from the highest percentages of *C. neoteretis*.

Time interval 13.2–12 ka shows highest total abundance of benthic foraminifers, up to 5994 tests/100 g dry sediment, around 13 ka concurrent with a decrease in the relative representation of all species besides *C. reniforme* which reaches up to 90% (Fig. 4). Such combination might indicate a short-lived establishment of harsh environmental conditions as this fast-reproducing species can take advantage also of rather unfavorable environments, like glacio-marine fjords (Korsun et al., 1994; Steinsund et al., 1994; Polyak et al., 2002) or even mud volcanos with methane seepage (Wollenburg and Mackensen, 2009). As revealed by cluster analysis the occurrence at 13 ka coincides with a major threshold in the composition of benthic foraminifers in general (Fig. 4). This time therefore likely marks a change from cold-water glacial-influenced assemblages to a series of assemblages representing the gradual transition to the modern assemblage. At 12.6 ka the benthic foraminiferal assemblage became more diverse with the dominance of *C. neoteretis* (up to 40–50%), *C. reniforme* and *E. clavatum*. After an intermittent abundance peak of *C. reniforme* around 12 ka, *C. neoteretis* completely disappeared from the record until about 7 ka.

Time interval 12–10.2 ka is characterized by some major changes in the composition of benthic foraminiferal assemblages. During the interval 12–11 ka, highest representation of *I. norcrossi*/*helenae*, *I. islandica*, and, especially, the only appearance of *N. labradoricum* in the core record, gives evidence of high seasonal productivity in association with the sea-ice marginal zone (Polyak et al., 2002; Wollenburg et al., 2004). In the later phase, between 11 and 10.2 ka, *C. reniforme* dominates the assemblage during times of the highest sedimentation rates.

Time interval 10.2–5.2 ka is rather poorly resolved due to the sharp drop in sedimentation rates (Figs. 2, 3). Still, growing representation of *Melonis barleeanus* and a gradual decrease of *C. reniforme* mark a transition to the modern-like foraminiferal assemblage (Fig. 5). *Melonis barleeanus* is a river-distant, relatively deep-water infaunal species which often occurs on soft grounds in troughs where it feeds on organic detritus (Caralp, 1989; Korsun et al., 1994; Steinsund et al., 1994; Polyak et al., 2002). Although it has been linked to Atlantic waters within troughs of the Barents Sea, *Melonis barleeanus* occurs there together with cold winter bottom waters and shelf-derived organic matter (Steinsund et al., 1994).

Time interval 5.2–2 ka is strongly different from assemblages before as it represents a modern-like community. It is dominated by arctic river-distal species *M. barleeanus*, *Islandiella* spp., and *Cibicides lobatulus*. The latter epifaunal species is usually regarded as an indicator of current activity (Polyak et al., 2002), but it can also give evidence for the presence of coarse particles on which it prefers to settle (Korsun et al., 1994; Steinsund et al., 1994). The percentage of species with epifaunal modes of life (*C. lobatulus*, *Astrononion gallowayi*, *Elphidium subarcticum*) reaches highest values during this time interval in accord with high IRD content (Fig. 3). Interestingly, simultaneously with the establishment of modern-like, deep-water assemblage, the share of river-proximal species also increases (Fig. 4). This is corroborated by the reappearance of *C. neoteretis* indicating the return of ADW at the site's water depth.

4.4. Planktic foraminifers

The polar species *N. pachyderma* sin. is by far the dominant species in the core, and its abundance variability mirrors the distribution of the total abundance of planktic foraminifers (Fig. 6). The peak abundance of planktic foraminifers is found at the base of the core (c. 17.2 ka), and in the same samples which contain only few benthic foraminifers. Most of these specimens are of rather small size with tests mainly occurring in the size-fraction 63–125 μm. This is notably the only interval within the core where the abundance of diverse subpolar species exceeds that of *N. pachyderma* sin. (Fig. 6).

Subpolar planktic foraminifers, which may be indicative of subsurface-derived Atlantic water inflow to the Laptev Sea (Bauch, 1999; Volkmann, 2000) already appeared at the very base of the core, at c. 17.6 ka. They are represented by several tests of *Globigerinita uvula* (Fig. 6). However, the most diverse assemblage of subpolar planktic foraminifers (>3000 tests/100 g sediment) is recorded slightly later, at c. 17.2 ka. The group is now comprised of *N. pachyderma* dex., *Globigerina bulloides*, *Globorotalia scitula*, *Globorotalia inflata*, *Globigerinita uvula*, *Globigerinita glutinata*, and *Turborotalita quinqueloba* (Fig. 6).

Until 15.4 ka subpolar planktic foraminifers occur periodically in low numbers, a few tests per sample. After 15.4 ka the total abundance of all planktic foraminifers increases and remains high until about 13 ka. The percentage of subpolar species is relatively high, 10–20%. Similar to the total abundance, taxonomic diversity of subpolar planktic foraminifers decreases at about the same time, i.e. 13 ka. Both facts point to the influence of freshened shelf water masses as a possible reason for observed changes. During the time interval 12–10.2 ka subpolar planktic foraminifers as well as *N. pachyderma* sin. are especially rare, probably, due to the strongest freshwater influence on the site.

In mid–late Holocene times, another increase in the total abundance of planktic foraminifers in the interval 5.2–2 ka marks a transition to the modern-like conditions. Unlike during lateglacial and deglacial times, taxonomic diversity of subpolar planktic foraminifers is low. Only three species, *N. pachyderma* dex., *G. bulloides* and *T. quinqueloba*, are present, the latter two being extremely rare (Fig. 6).

4.5. Ostracods

With regard to the ostracod components in core PS51/154, we concentrate on the distribution of different ecological groups (Fig. 7) and representatives of the North Atlantic group, i.e., species found on shelf-upper slope in both North Atlantic and Arctic oceans, together with the Arctic cold-water species *Krithe glacialis* (Fig. 8); a more detailed record of all ostracod species from core PS51/154 is given in Stepanova et al. (in press). The ecology of ostracod species has gained considerably less attention compared to foraminifers. Therefore, the relationship between the group of North Atlantic ostracods and the inflows of ADW is rather provisional. These species are restricted to the continental slope in the marginal Arctic Ocean seas, thus implying their association with the ADW (Stepanova et al., 2003, 2004, 2007; Cronin et al., 2010), whereas in the North Atlantic they occur at considerably larger water depths (Whatley et al., 1996; Alvarez Zarikian et al., 2009).

The oldest finding of ostracod valves refers to the same sediment layer (c. 17.2 ka) where also the abundant but small-sized subpolar planktic foraminifers were recognized. This finding includes two North Atlantic species, *C. laptevensis* and *C. paralatissimum* (Fig. 8). During the time interval 15.4–10.2 ka, ostracod assemblages demonstrate the highest diversity as they include the full range of ecological groups from relatively deep-water North Atlantic species to species indicative of brackish- and even freshwater environments (Fig. 7). This gives evidence of the proximity of the Siberian paleo-coast relative to the site as well as fluvial influence on one hand, and the presence of cold and marine open-sea waters, on the other. Abundance peaks of ostracods at about 14.7–14.5, 13 and 12 ka correlate with the peaks of benthic foraminifers implying either high surface water productivity or, in contrary, a better preservation of calcareous tests due to more permanent sea ice and low input of organic matter to bottom sediments (Wollenburg et al., 2004; Schell et al., 2008).

Continuous presence of North Atlantic species since 15.4 ka suggests constant influence of ADW on the western Laptev Sea continental slope. The relative abundance of these species is high during time-intervals 15.4–14.7 and 13–12 ka, but diminishes during subsequent periods of stronger fluvial influence and growing seasonal productivity 14.7–13 and 12–10.2 ka. Thus, we assume that from the ecological point of view these species are indicators of more saline, cold-water environments with weak water stratification. Like in the case with subpolar planktic foraminifers, North Atlantic ostracods are more taxonomically diverse prior to c. 10.2 ka than in the Holocene. Several species, like *C. paralatissimum*, *C. pseudomontrosiense*, *C. inflatum*, *B. constricta*, *P. caudata* disappear at this time level. Others persist in the Holocene, and the only North Atlantic species introduced as new is *C. perlaria*.

Since 5.2 ka the percentage of North Atlantic ostracods decreases, and shallow-water marine species *Sarsicytheridea punctillata* (Stepanova et al., in press) becomes dominant. Simultaneously, the percentage of inner-shelf euryhaline species also increases. These species are likely being ice-rafted to this distant locality (Stepanova et al., in press).

5. Past environmental changes in the western Laptev Sea in relation to Atlantic water mass influence

There is ample evidence for a continuous inflow of Atlantic waters to the Arctic Ocean, namely along the eastern Nordic seas and Fram Strait to the northern Barents Sea margin, during various phases of the last 150 ka (Knies et al., 1999), including the Last Glacial Maximum (LGM), the last deglaciation and Holocene (Bauch et al., 2001a; Nørgaard-Pedersen et al., 2003; Wollenburg et al., 2004; Ślubowska et al., 2005; Rasmussen et al., 2007; Ślubowska-Woldengen et al., 2007, 2008). Due to the complicated history of regional sea-level changes, glaciation and deglacial processes, the influx of ADW to the troughs of the northern Barents and Kara seas after the LGM was intermittent (Hald et al., 1999; Lubinski et al., 2001; Ivanova et al., 2002). Core PS51/154 from the upper Laptev Sea continental slope is located in the vicinity of the exposed Laptev Sea shelf which was not glaciated during the LGM (Fig. 1; Svendsen et al., 2004), but which was always connected to the global ocean. It is therefore well-suited to record inflow patterns of ADW through time for both, lateglacial and early deglacial periods when the only pathway with the FSBW existed, and those times since 12–10 ka when the BSBW pathway to the troughs was re-established (Polyak and Mikhailov, 1996; Lubinski et al., 2001).

5.1. Time interval c.17.6–15.4 ka

Already at the very base of core PS51/154 sediment record with extrapolated age of 17.6 ka rare tests of subpolar planktic foraminifer *G. uvula* give evidence for ADW influence on the western Laptev Sea continental slope. During the lateglacial and early deglacial period single subpolar planktic foraminifers occur sporadically, except for an outstanding short-lived event at c.17.2 ka, when their diversity and abundance increase drastically (Figs. 6, 9). Co-occurrence of benthic microfossils including *C. neoteretis* and North Atlantic ostracods, which are otherwise almost absent prior to 15.4 ka, indicates concurrent amelioration of bottom water environment at the site likely due to the influence of ADW. However, the general absence of benthic microfossils during 17.6–15.4 ka (which was not the result of dissolution) and the occurrence of authigenic concretions point to predominantly anaerobic conditions at the sea floor that were unfavorable for benthos.

The overall glacial-like environment of the studied site at the upper continental slope prior to 15.4 ka represented a cold-water marine setting, with closely located coastline on exposed permafrost shelf (Hubberten et al., 2004). Low TOC content in the sediments suggests there was little supply of organic matter from the frozen mainland, also because of reduced river discharge under cold and dry climatic conditions (Tarasov et al., 1999). Predominance of cold-water euryhaline dinocysts and the absence of autotrophic species indicate diminished biological production due to heavy sea-ice conditions (Fig. 9; Klyuvitkina, 2007; Klyuvitkina et al., 2009). However, the four IRD peaks document more seasonally open-water conditions with drifting icebergs, whereas subsequent periods of meltwater-induced stratification and concretion formation evidence more severe sea ice covered environment in summer (Taldenkova et al., 2010).

In winter, offshore winds blowing from the cold permafrost mainland should have maintained open water coastal polynyas. Given the proximity of the coastline and the steepness of submarine slope (Fig. 1), the past environment likely resembled the modern regions of the NW Laptev Sea close to Severnaya Zemlya. Here, active sea-ice formation in polynyas produces cascading of dense saline cold waters which ventilate bottom waters on the slope and facilitate upwelling of ADW (Ivanov and Golovin, 2007). Also, similarly to modern observations, stronger offshore winds forced the core of ADW to move onshore (Dmitrenko et al., 2006, 2010). It could well be the case that periodically strong upwellings of ADW to the site of core PS51/154, like the c. 17.2 ka event correlative with IRD peak, resulted from such active water circulation in the former nearcoastal zone. In lateglacial and early deglacial times, Atlantic water in the Nordic seas was flowing as a strong subsurface current beneath the polar meltwater layer and transported considerable warmth to the Arctic Ocean (Bauch et al., 2001a; Rasmussen et al., 2007). As a subsurface inflow it continued further into the Arctic along the continental slope and definitely also reached the Laptev Sea. The fact that it carried abundant "exotic" warm-water subpolar planktic foraminifers suggests that it was not undergoing considerable alterations on the way. Between c. 17.6 and 15.4 ka global sea level was more than 100 m lower than now (Fairbanks, 1989). Therefore, the core site was located at water depths of about 160–170 m, probably, above the upper limit of the ADW layer. As a result, only periodically did strong upwellings advect these waters upslope to reach the site.

5.2. Time interval 15.4–14.7 ka

During this time interval environmental setting resembled that of the previous period in terms of proximity to the Siberian coastline and cold-water predominantly ice-covered conditions. Proximity to the coast is evidenced by the prominent sand slide event at 15 ka with freshwater and brackishwater ostracods and river-proximal foraminifers. Growing but still low TOC content and the absence of autotrophic species among dinocysts (Fig. 9; Klyuvitkina, 2007; Klyuvitkina et al., 2009) indicate reduced surface water productivity due to heavy seasonal sea-ice cover. The same is generally suggested by the taxonomic composition of benthic assemblages where cold-water arctic species predominate among benthic foraminifers (*C. reniforme*) and ostracods (*K. glacialis*).

The major change relates to the drastic decrease in IRD and increase in benthic and planktic microfossils. Low IRD content suggests that iceberg-rafting almost ceased due to the inland retreat and melting of ice caps (Taldenkova et al., 2010). Continuous presence of benthic organisms and relatively high total abundance imply amelioration of bottom water environment, which was most likely due to the growing influence of ADW. The latter might have been also induced by local upwelling events as indicated by the high percentages of *S. feylingi* (Knudsen et al., 2008). Upwelling of ADW to the site location occurred frequently as evidenced by almost continuous presence of *C. neoteretis*, diverse subpolar planktic foraminifers and North-Atlantic ostracods (Fig. 9). In the eastern Nordic seas strong northward advection of Atlantic water in the subsurface layer occurred in the stratified water column beneath the surface meltwater-freshened layer (Bauch et al., 2001a; Rasmussen et al., 2007). In cores JM03-373 and JM02-460 to the southwest from Spitsbergen (Fig. 1), the relative abundance of *C. neoteretis* reached up to 40% (Rasmussen et al., 2007). This subsurface inflow was rather strong also north of Spitsbergen, where the percentage of *C. neoteretis* in core NP94–51 (Fig. 1) was 20–25% (Fig. 9; Ślubowska et al., 2005; Ślubowska-Woldengen et al., 2008). The relative abundance of *C. neoteretis* in core PS51/154 in the western Laptev Sea is comparable, up to 20–25%, thus indicating the far reaching rather unmodified subsurface inflow of ADW with its northern branch (FSBW). The pathway of ADW through the Barents shelf (BSBW) was likely still non-existent (Lubinski et al., 2001).

5.3. Time interval 14.7–13.2 ka

This period corresponds to the warm Bølling–Allerød interstadial that abruptly started at 14.7 ka as indicated by the Greenland ice core data (Fig. 9; Steffensen et al., 2008). The sea-level rose above −100 m water depth that led to the onset of the Laptev shelf flooding (Fairbanks, 1989; Bauch et al., 2001b). Due to climate amelioration, active coastal erosion, increased river runoff and still rather close location of the coastline to the site of core PS51/154 sedimentation rates increased, as did the amount of terrestrial organic matter (Fig. 3). Stronger fluvial influence upon the site likely induced by climate warming is primarily evidenced by the dominance of *E. clavatum* among benthic foraminifers which took advantage of thriving in more stratified and turbid waters. Seasonal ice cover remained rather heavy as indicated by high percentages of *S. loeblichi*, *E. clavatum* among benthic foraminifers and *K. glacialis* among ostracods. However, the growing abundance of *Islandiella* spp. since 14.4 ka, high abundance of planktic foraminifers including numerous subpolar species manifest a shift to more seasonally open conditions as compared to previous times.

The inflow of subsurface ADW was strong and constant as seen from the highest percentages of *C. neoteretis* sometimes rising up to 60% (Fig. 9). Due to the rapidly increasing water depths, the core site probably became located within the upper part of the ADW layer. In the west, the subsurface flow of Atlantic waters was strong along the western Barents Sea margin and affected the shelf areas (Ebbesen et al., 2007; Rasmussen et al., 2007; Ślubowska-Woldengen et al., 2008). Relative representation of *C. neoteretis* in cores JM03-373, JM02-460 and JM02-440 was around 20%. Even higher values, up to 50–60%, were recorded north of Svalbard in core NP94-51 (Fig. 9; Ślubowska et al., 2005; Ślubowska-Woldengen et al., 2008) and in cores from Franz Victoria and St. Anna troughs (Lubinski et al., 2001). The remarkable similarity in the outline of *C. neoteretis* records in the western Laptev Sea and Northern Spitsbergen shelf demonstrates that it was the same subsurface inflow of ADW with the FSBW that continued largely unmodified along Eurasian continental slope (Fig. 9). Although the troughs in the northern Barents and Kara seas were deglaciated by about 15 ka, the timing of the establishment of another pathway of Atlantic waters through the Barents shelf remains questionable (Lubinski et al., 2001). In the southwestern Barents Sea shelf, sporadic occurrence of *C. neoteretis* and the absence of planktic foraminiferal fauna in cores JM05-085 and PSh-5159 (Fig. 1) prior to 13.8 ka allows assuming brief influence of Atlantic waters at the seafloor with gradual intensification afterwards between 13.8 and 12.7 ka (Aagard-Sørensen et al., 2010; Chistyakova et al., 2010).

5.4. Time interval 13.2–12 ka

This time interval largely corresponds to the cold Younger Dryas period characterized by freshwater-induced weakening of the North Atlantic thermohaline circulation and, therefore, reduced influence of Atlantic waters in the eastern Nordic seas and the Barents Sea (Bauch et al., 2001a; Bradley and England, 2008; Ślubowska-Woldengen et al., 2008). In the western Laptev Sea it is distinguished by drastic changes in lithology and composition of benthic assemblages. Reduction in sedimentation rates during the whole interval is combined with the drop in TOC and C/N after 13 ka. Total abundances of all microfossil groups peak at 13 ka, and to a lesser degree at 12 ka. The largest peak at 13 ka is represented by a single dominant species *C. reniforme* among benthic foraminifers concurrent with the disappearance of ADW-indicative species *C. neoteretis*.

It is likely that the abundance peaks at 13 ka and still high TOC content between 13.2 and 13 ka are the result of environmental development during the Bølling–Allerød period that culminated in longer seasonally ice-free conditions and surface water warming. Indeed, the data on aquatic palynomorphs, especially the first appearance of autotrophic species among dinocysts at 13 ka confirms this interpretation (Fig. 9; Klyuvitkina, 2007; Klyuvitkina et al., 2009).

However, the “monospecific” composition of the benthic foraminiferal assemblage dominated by the Arctic opportunistic species *C. reniforme* at 13 ka gives evidence for a shift to harsh environmental conditions. It could be initiated by a strong influx of freshwater that produced a stratified water column in the coastal region and displaced the ADW water layer offshore. Strong freshening of the upper water layer at around 13 ka was recorded by the negative shift in $\delta^{18}O$ composition of planktic foraminifers *N. pachyderma* sin. from nearby core PS2458 on the eastern Laptev Sea continental slope in front of the former Lena River mouth (Fig. 1; Spielhagen et al., 2005). It was proposed that the freshwater influx resulted from an outburst of river water after the disappearance of a dam across the Lena River formed by an extension of mountain glaciers (Spielhagen et al., 2005). Similar prominent $\delta^{18}O$ minimum in planktic foraminifers was identified at about 13 ka further eastward at the Chukchi margin. It was likely caused by meltwater discharge from the Laurentide ice sheet possibly associated with the flooding from Lake Agassiz (Polyak et al., 2007). These freshwater inputs to the Arctic Ocean in combination with sea-level rise and intensification of water circulation also due to the Bering Strait opening close to 13 ka resulted in the massive evacuation of the thick multiyear ice to the North Atlantic thus contributing to initiation of the Younger Dryas event (Bradley and England, 2008; England and Furze, 2008).

As a consequence of 13 ka freshwater event(s) the seasonal ice cover at the studied location became heavier. Sedimentation rates and TOC content decreased because of lower primary productivity and weaker coastal erosion. The total abundance of microfossils, especially planktic foraminifers, decreased between about 12.7 and 12 ka. However, at the same time the prominent peak in the percentage of *C. neoteretis* of up to 40–50% shows that ADW likely affected the bottom water layer below the freshened and stratified water column (Fig. 9). This peak in *C. neoteretis* in the western Laptev Sea does not correlate to the evidence from the “upstream” regions in the northern Barents and Kara troughs (Lubinski et al., 2001) and around Svalbard (Fig. 9; Ślubowska et al., 2005; Ślubowska-Woldengen et al., 2007, 2008) which all indicate reduced inflow of ADW during this time. The same is true for the southwestern Barents Sea shelf. Although the influence of Atlantic waters gradually intensified there, the continued inflow reflected by similarly high representation of *C. neoteretis* began at 11.9–11.8 ka (Aagard-Sørensen et al., 2010; Chistyakova et al., 2010). It might be assumed that the observed *C. neoteretis* peak in the western Laptev Sea is a result of specific past regional development.

5.5. Time interval 12–10.2 ka

Although rather unstable, the period of the late Younger Dryas–Holocene transition corresponding to the times of summer insolation maximum (Berger and Loutre, 1991) is characterized by evident climate-induced surface water warming at the western Laptev Sea continental slope as reflected by microfossils. Especially between 12 and 11 ka, relatively high total abundances of benthic microfossils in combination with increased percentages of such species as *I. norcrossi/helenae*, *I. islandica*, and the single peak of *N. labradoricum* give evidence for high seasonal productivity. These species are known to prefer fresh phytodetritus associated with sea-ice marginal zone (Polyak et al., 2002; Wollenburg et al., 2004). It is likely, that during 12–11 ka the seasonal drift ice limit was located close to the core site. High seasonal productivity is corroborated by the highest TOC values accompanied by a decrease in C/N ratio thus indicating growing contribution of marine organic matter. The observed fragmentation of foraminiferal tests and a decrease in $CaCO_3$ content likely result from dissolution produced by corrosive bottom waters. The latter are linked to sea-ice production and remineralization of organic matter occurring in the regions with seasonal sea-ice cover and enhanced summer productivity (Steinsund and Hald, 1994; Bauch et al., 2001a; Wollenburg et al., 2004; Schell et al., 2008). Also, the percentage of autotrophic species of dinocysts increases considerably, especially after 11 ka, as does the relative abundance of North Atlantic species *O. centrocarpum* (Fig. 9; Klyuvitkina and Bauch, 2006; Klyuvitkina, 2007; Klyuvitkina et al., 2009). Palynological data evidence that regional climate conditions were warmer than present after 11.3 ka and until 5.3 ka (Naidina and Bauch, 2011).

Both, the highest TOC values and sedimentation rates result from active coastal erosion in the course of extensive outer and middle shelf flooding by rapidly rising sea level (Bauch et al., 1999, 2001b; Taldenkova et al., 2005, 2008). Together with increasing fluvial supply due to climate warming this caused formation of freshened shelf water mass that actively interacted with the open-sea waters. The resulting freshening and stratification of the open-sea waters on the upper continental slope created environmental conditions that were unfavorable for planktic foraminifers and *C. neoteretis* (Lubinski et al., 2001). The latter species is completely absent in our record during 12–10.2 ka. It is possible to assume that ADW was shifted offshore away from the core site.

In the central Nordic seas and western Barents shelf margin, the reconstructed warmest surface waters after 11 ka are assumed to indicate enhanced inflow of surface Atlantic waters (Sarnthein et al., 2003; Hald et al., 2004; Ebbesen et al., 2007; Hald et al., 2007; Rasmussen et al., 2007; Ślubowska-Woldengen et al., 2007, 2008). Since warm Atlantic water flowing into the Nordic seas suffers substantial heat loss on its way to the north, at the northern Svalbard margin the inflow of Atlantic water is recorded mostly as an increase in salinity and productivity, whereas *C. neoteretis* content is rather low in the cores westward and northward from Svalbard (Ślubowska et al., 2005; Rasmussen et al., 2007; Ślubowska-Woldengen et al., 2007, 2008). However, it might be also due to the ecological preferences of *C. neoteretis* which is rather associated with chilled subsurface than surface Atlantic waters (Wollenburg and Mackensen, 1998; Osterman et al., 1999; Lubinski et al., 2001; Wollenburg et al., 2004).

In contrast, the relative abundance of *C. neoteretis* was high in the southwestern Barents Sea after 11.8–11.5 ka reaching up to 50–60% in core PSh5159 (Aagard-Sørensen et al., 2010; Chistyakova et al., 2010). Here at 11–9.8 ka, Atlantic water was in the subsurface overlain by cold freshened surface water and extensive seasonal sea ice cover (Chistyakova et al., 2010; Risebrobakken et al., 2010), the conditions which are favorable for *C. neoteretis*. However, further northward in Franz Victoria and St. Anna troughs the subsurface and bottom waters were apparently occupied by cold BSBW after 11 ka, as suggested by the very low abundance of *C. neoteretis* and specific changes in the isotopic composition of planktic and benthic foraminiferal tests (Lubinski et al., 2001). Continuous and strong inflow of Atlantic water to the southwestern Barents Sea might be related to the changes in atmospheric circulation preferentially pushing Atlantic water in the lateral direction to the Barents Sea (Lubinski et al., 2001). Inference about stronger westerlies during early–mid Holocene gets support in the eastward shift of subsurface Arctic water recorded in the core from the Vøring plateau (Risebrobakken et al., 2003). Further distribution of Atlantic waters on the Barents shelf was guided by overdeepening of the northern Barents Sea caused by a thicker glacial load in the north compared to its southern part (Lubinski et al., 2001). Both processes explain the dominance of cold BSBW in the northern troughs. The enhancement of BSBW influence in the troughs might be also tentatively related to the disappearance of *C. neoteretis* in core PS51/154 after 12 ka as this site in the western Laptev Sea experiences combined influence of both Atlantic water branches, and *C. neoteretis* is largely restricted to FSBW (Lubinski et al., 2001).

5.6. Time interval 10.2–5.2 ka

This time interval in core PS51/154 is poorly resolved due to the sharp break in sedimentation rates after the flooding of outer and middle shelf completed, and depositional centers shifted farther inland (Bauch et al., 1999, 2001b). The core site gradually became located at the modern water depth and at a considerable distance from the coast. The low total abundances of all groups of microfossils and the decreasing representation of “phytodetritus” species might be an indication of offshore displacement of the average summer drift ice margin from the core site due to progressive surface water warming. This assumption is corroborated by the near absence of IRD and ice-rafted microfossil species from the inner shelf region, i.e. river-proximal foraminifers and euryhaline/brackishwater ostracods. These species, together with coarse sediment fragments, are entrained into the newly formed ice in the nearshore zone during autumn storms and brought to the seasonal drift ice margin, from where they start their drift through the ocean partly melting away on the way (Reimnitz et al., 1987, 1994; Eicken et al., 1997). This implies that the colder the summer is, the farther onshore is the seasonal drift ice limit, and more IRD and shallow-water microfossils are released next summer within the outer Laptev Sea. In the surface samples from the Laptev and Kara seas we observed two maxima in the distribution of euryhaline ostracods, the main one in the inner shelf zone, where these species predominate, and a second subordinate one on the outer shelf and upper continental slope, where relatively deep-water species are dominant (Stepanova et al., 2003, 2007). In the Barents Sea cores, it has been also observed that the distribution of benthic foraminifers largely relates to migrations of sea-ice margin and Polar front, and that the Holocene warming deduced from isotopic data is accompanied by decreasing abundance of foraminifera (Ivanova et al., 2002).

It might be concluded that the seasonal sea-ice marginal zone shifted northward from core site PS51/154 during 11–7 ka. As the Laptev Sea was not subject to meltwater influence at this time, this early Holocene optimum was likely due to surface water warming in accordance with the peak summer insolation. During most of the early Holocene the sea-ice cover was strongly reduced in the Arctic with periods of ice-free summers even in the central Arctic Ocean (Jakobsson et al., 2010; Polyak et al., 2010). Warm surface water conditions at the site are also evidenced by high percentages of autotrophic dinocyst species and high relative abundance of *O. centrocarpum* (Fig. 9; Klyuvitkina, 2007; Klyuvitkina et al., 2009). Pollen spectra suggest that climate conditions between 10.3 and 8 ka were not only warmer but also more humid than now (Naidina and Bauch, 2011).

In the North Atlantic and the Barents Sea both meridional and lateral inflows of warm Atlantic water remained strong (Duplessy et al., 2001;

Lubinski et al., 2001; Ebbesen et al., 2007; Rasmussen et al., 2007; Ślubowska-Woldengen et al., 2007, 2008; Aagard-Sørensen et al., 2010; Chistyakova et al., 2010). BSBW dominated the northern troughs until 8.3 ka. Then FSBW returned and occupied the water column in the troughs down to the sea floor during the Holocene thermal optimum 7.8–6.8 ka (Duplessy et al., 2001; Lubinski et al., 2001; Duplessy et al., 2005). Thereafter, due to continuing shoaling a separation between Atlantic-derived water masses in the Barents Sea resulted in more FSBW in Franz Victoria trough, and more BSBW in St. Anna trough (Lubinski et al., 2001).

At about 7 ka the modern-type circulation started to evolve in the Nordic seas with strong inflow of Atlantic water in the east to the Arctic Ocean and outflow of the polar waters along Greenland (Bauch et al., 2001a). By this time the last remaining Laurentide ice sheet vanished, and this led to the enhancement of overturning strength of the thermohaline circulation (Renssen et al., 2009). A general cooling trend since about 7 ka is recorded along the western Barents Sea margin and has been interpreted as decrease in heat advection by Atlantic water during times of diminishing northern insolation intensity (Sarnthein et al., 2003; Hald et al., 2004; Ebbesen et al., 2007; Rasmussen et al., 2007; Ślubowska-Woldengen et al., 2007, 2008). The combination of strong advection of chilled ADW and climate cooling is manifested in our record by enhanced IRD input since 7.2 ka (due to the re-growth of ice caps on Severnaya Zemlya) and simultaneous re-appearance of *C. neoteretis* (Fig. 9; Taldenkova et al., 2010).

5.7. Time-interval 5.2–0.6 ka

During this time interval environmental changes became increasingly influenced by climate variables other than sea-level-driven factors. Climate cooling is manifested in our record by enhancement of iceberg-rafting due to regrowth of ice caps on Severnaya Zemlya (Taldenkova et al., 2010). The better resolved record of IRD in nearby core PS51/159 on the outer shelf (Fig. 1) showed that the IRD peaks are centered at 7.2, 6.4, 5.4, 3, and 2 ka with the strongest iceberg production recorded between 5.4 and 2 ka in both cores (Fig. 9). In core PS51/154 a small IRD peak is also seen at c. 0.6 ka. This millennial-scale variability in IRD input might be related to overregional changes in atmospheric circulation. These are variations in the mode of the North Atlantic (NAO) and Arctic (AO) oscillations similar to millennial-scale variability in the intensity of westerlies associated with the NAO (Duplessy et al., 2005) or millennial-scale climate-induced shifts in sea-ice drift pathways, freshwater discharge and its spatial distribution controlled by the changes in the phase of AO/NAO (Darby and Bischof, 2004; Darby et al., 2006).

Due to the low resolution of core PS51/154 record it is difficult to trace similar climate-controlled variability in the ADW inflows to the western Laptev Sea continental slope. However, it is evident that the peaks in *C. neoteretis* percentages and abundance of subpolar planktic foraminifers and North Atlantic ostracods generally correlate with the observed IRD peaks (Fig. 9). The character of ADW inflows in the mid–late Holocene and the overall environmental setting differ from deglacial times. The percentage of *C. neoteretis* does not exceed 10% compared to the average 20–30% during deglacial times (Fig. 9). Taxonomic diversity of subpolar planktic foraminifers and North Atlantic ostracods is lower. The possible explanation is that instead of a strong unmodified subsurface inflow of chilled ADW with FSBW during deglacial times, in the mid–late Holocene both branches of ADW contributed to the flow reaching the Laptev Sea.

The overall environmental setting was also different. Flooding of the whole vast Laptev shelf resulted in less freshwater influence on the distant regions on the western upper continental slope. Progressively decreasing TOC content and C/N ratio result from reduction in terrestrial organic matter supply and increasing contribution of marine organic matter, especially after 3 ka. Drastic changes occurred in the benthic foraminiferal assemblage, where *M. barleeanus* became dominant; a relatively deep-water species thriving on slightly altered organic matter and thus restricted to the distal areas with periodical delivery of organic matter. High relative abundance of species with attached mode of life is likely a result of increasing abundance of coarse IRD fragments in the sediments. Growing representation of river-proximal foraminifers, and re-appearance of euryhaline ostracods which were almost absent during times of the early Holocene surface water warming, indicate onshore shift of the summer drift ice margin and surface water cooling. All together, these features characterize establishment of the modern-like environment with the variability of environmental parameters largely induced by atmospheric forcing.

6. Conclusions

A new, high-resolution reconstruction of paleoceanographic events at the western Laptev Sea upper continental slope is correlated with those recorded in the western regions located on the pathway of ADW from the North Atlantic.

- Subsurface ADW masses were continuously present at the western Laptev Sea continental margin throughout the recorded time span, i.e. since c. 17.6 ka.
- Until around 13 ka the ADW inflow to the Laptev Sea was an almost unmodified continuation of the strong subsurface flow of chilled FSBW water along the northern Eurasian continental slope. This is judged from abundant diverse subpolar planktic foraminifers and similarly high representation of *C. neoteretis* in the waters around Svalbard and in the western Laptev Sea. With the exposed shelf, the western Laptev Sea upper continental slope represented a cold-water marine setting with heavy seasonal sea-ice cover and frequent, wind-induced coastal polynyas in winter that facilitated upwelling of ADW. Gradual climate amelioration since 14.7 ka resulted in a longer seasonal ice-free period and a stronger fluvial influence.
- Between 13 and 7 ka environmental changes at the studied site in the western Laptev Sea upper continental slope were largely driven by sea-level factors, i.e. active shelf flooding, coastal erosion and establishment of freshened shelf water mass. The resulting freshening and stratification of the open-sea waters forced the ADW flow to shift offshore away from the core site. This is suggested by the disappearance of *C. neoteretis* from the record between 12 and 7 ka. The absence of *C. neoteretis*, which is largely restricted to the FSBW, could be also tentatively related to enhancement of BSBW influence in the northern Barents and Kara troughs during the early Holocene. The studied site was located within the sea-ice marginal zone at 12–11 ka as seen from the only peak of *Nonion labradoricum* and high percentages of other "phytodetritus" species. Later, during the early Holocene climate warming, the sea-ice marginal zone was displaced further offshore.
- Enhanced ADW inflow since 7 ka correlates with the establishment of a modern-like environment, climate cooling, enhanced iceberg production and southward retreat of the seasonal drift-ice margin. ADW inflow during mid-late Holocene differed from deglacial times because of the combined influence of both ADW branches.

Supplementary data to this article can be found online at http://dx.doi.org/10.1016/j.marmicro.2012.06.007.

Acknowledgments

We thank the team from the Leibniz Laboratory (Kiel) for conducting AMS^{14}C measurements and T. Mueller-Lupp for providing geochemical data. We acknowledge the assistance of collaborators of the Otto Schmidt Laboratory for Polar and Marine Sciences (OSL) in sample processing. We thank M. Ślubowska-Woldengen with her co-authors for providing us with their original data. This research was supported by the BMBF and Russian Ministry for Education and Science (OSL fellowship projects), the Russian Foundation for Basic

Research (projects 08-05-00849 and 11-05-01091), and INTAS (project 03-51-6682).

References

Aagard-Sørensen, S., Husum, H., Hald, M., Knies, J., 2010. Paleoceanographic development in the SW Barents Sea during the late Weichselian–Early Holocene transition. Quaternary Science Reviews 29 (25–26), 3442–3456.

ACIA, 2005. Arctic Climate Impact Assessment. Cambridge University Press, Cambridge. Available from: http://www.acia.uaf.edu.

Alvarez Zarikian, C.A., Stepanova, A.Yu., Grützner, J., 2009. Glacial-interglacial variability in deep sea ostracod assemblage composition at IODP Site U1314 in the subpolar North Atlantic. Marine Geology 258, 69–87.

Bauch, H.A., 1999. Planktic foraminifera in Holocene sediments from the Laptev Sea and the Central Arctic Ocean: species distribution and paleobiogeographical implication. In: Kassens, H., Bauch, H.A., Dmitrenko, I., Eicken, H., Hubberten, H.-W., Melles, M., Thiede, J., Timokhov, L. (Eds.), Land-Ocean Systems in the Siberian Arctic: Dynamics and History. Springer, New York, pp. 601–614.

Bauch, H.A., Kassens, H., 2005. Arctic Siberian shelf environments — an introduction. Global and Planetary Change 48 (1–3), 1–8.

Bauch, H.A., Kassens, H., Erlenkeuser, H., Grootes, P.M., Thiede, J., 1999. Depositional environment of the Laptev Sea (Arctic Siberia) during the Holocene. Boreas 28, 194–204.

Bauch, H.A., Erlenkeuser, H., Spielhagen, R.F., Struck, U., Matthiessen, J., Thiede, J., Heinemeier, J., 2001a. A multiproxy reconstruction of the evolution of deep and surface waters in the subarctic Nordic seas over the last 30,000 yr. Quaternary Science Reviews 20, 659–678.

Bauch, H.A., Mueller-Lupp, T., Taldenkova, E., Spielhagen, R.F., Kassens, H., Grootes, P.M., Thiede, J., Heinemeier, J., Petryashov, V.V., 2001b. Chronology of the Holocene transgression at the North Siberian margin. Global and Planetary Change 31, 125–139.

Berger, A., Loutre, M.F., 1991. Insolation values for the climate of the last 10 million years. Quaternary Science Reviews 10, 297–317.

Boucsein, B., Stein, R., 2000. Particular organic matter in the surface sediments of the Laptev Sea (Arctic Ocean): application of maceral analysis as organic-carbon-source indicator. Geology 162, 573–586.

Bradley, R.S., England, J.H., 2008. The Younger Dryas and the sea of ancient ice. Quaternary Research 70, 1–10.

Bujak, J.P., 1984. Cenozoic dinoflagellate cysts and acritarchs from the Bering Sea and northern North Pacific, DSDP Leg 19. Micropaleontology 30 (2), 180–212 (pls. 1–4).

Caralp, M.H., 1989. Size and morphology of the benthic foraminifer Melonis barleeanum: relationships with marine organic matter. Journal of Foraminiferal Research 19 (3), 235–245.

Carmack, E., Barber, D., Cristensen, J., Macdonald, R., Rudels, B., Sakshaug, E., 2006. Climate variability and physical forcing of the food webs and the carbon budget on panarctic shelves. Progress in Oceanography 71, 145–181.

Chistyakova, N.O., Ivanova, E.V., Risebrobakken, B., Ovsepyan, E.A., Ovsepyan, Ya.S., 2010. Reconstruction of the Postglacial environments in the southwestern Barents Sea based on foraminiferal assemblages. Oceanology 50 (4), 573–581.

Comiso, J.C., Parkinson, C.L., Gersten, R., Stock, L., 2008. Accelerated decline in the Arctic sea ice cover. Geophysical Research Letters 35, L01703. http://dx.doi.org/10.1029/2007GL031972.

Cronin, T.M., Gemery, L.J., Brouwers, E.M., Briggs Jr., W.M., Wood, A., Stepanova, A., Schornikov, E.I., Farmer, J., Smith, K.E.S., 2010. Arctic Ostracode Database 2010. IGBP PAGES/World Data Center for Paleoclimatology. Data Contribution Series # 2010–081. NOAA/NCDC Paleoclimatology Program, Boulder CO, USA. ftp://ftp.ncdc.noaa.gov/pub/data/paleo/contributions_by_author/cronin2010/cronin2010.txt.

Darby, D.A., Bischof, J.F., 2004. A Holocene record of changing Arctic Ocean ice drift analogous to the effects of the Arctic Oscillations. Paleoceanography 19, PA1027. http://dx.doi.org/10.1029/2003PA000961.

Darby, D.A., Polyak, L., Bauch, H.A., 2006. Past glacial and interglacial conditions in the Arctic Ocean and marginal seas — a review. In: Wassman, P. (Ed.), Structure and Function of Contemporary Food Webs on Arctic Shelves — A Pan-Arctic Comparison: Progress in Oceanography, 71, pp. 129–144.

Dmitrenko, I.A., Hoelemann, J., Kirillov, S.A., Berezovskaya, S.L., Kassens, H., 2001. The role of barotropic sea-level changes in formation of current regime on the eastern Laptev Sea shelf. Doklady Earth Sciences 377 (1), 1–8 (in Russian).

Dmitrenko, I.A., Polyakov, I.V., Kirillov, S.A., Timokhov, L.A., Simmons, H.L., Ivanov, V.V., Walsh, D., 2006. Seasonal variability of Atlantic water on the continental slope of the Laptev Sea during 2002–2004. Earth and Planetary Science Letters 244, 735–743.

Dmitrenko, I.A., Polyakov, I.V., Kirillov, S.A., Timokhov, L.A., Frolov, I.E., Sokolov, V.T., Simmons, H.L., Ivanov, V.V., Walsh, D., 2008. Toward a warmer Arctic Ocean: spreading of an early 21st century Atlantic water warm anomaly along the Eurasian Basin margin. Journal of Geophysical Research 113, C05023. http://dx.doi.org/10.1029/2007JC004158.

Dmitrenko, I.A., Kirillov, S.A., Tremblay, L.B., Bauch, D., Hölemann, J.A., Krumpen, T., Kassens, H., Wegner, C., Heinemann, G., Schröder, D., 2010. Impact of the Arctic Ocean Atlantic water layer on Siberian shelf hydrography. Journal of Geophysical Research 115, C08010. http://dx.doi.org/10.1029/2009JC006020.

Duplessy, J.C., Ivanova, E.V., Murdmaa, I.O., Paterne, M., Labeyrie, L., 2001. Holocene palaeoceanography of the Northern Barents Sea and variations of the northward heat transport by the Atlantic Ocean. Boreas 30, 2–16.

Duplessy, J.C., Cortijo, E., Ivanova, E., Khusid, T., Labeyrie, L., Levitan, M., Murdmaa, I., Paterne, M., 2005. Paleoceanography of the Barents Sea during the Holocene. Paleoceanography 20, PA4004. http://dx.doi.org/10.1029/2004PA001116.

Ebbesen, H., Hald, M., Eplet, T.H., 2007. Lateglacial and early Holocene climatic oscillations on the western Svalbard margin, European Arctic. Quaternary Science Reviews 26, 1999–2011.

Eicken, H., Reimnitz, E., Alexandrov, V., Martin, T., Kassens, H., Viehoff, T., 1997. Sea-ice processes in the Laptev Sea and their importance for sediment export. Continental Shelf Research 17 (2), 205–233.

England, J.H., Furze, M.F.A., 2008. New evidence from the western Canadian Arctic Archipelago for the resubmergence of Bering Strait. Quaternary Research 70, 60–67.

Fairbanks, R.G., 1989. A 17,000-year glacio-eustatic sea level record: influence of glacial melting rates on the Yonger Dryas event and deep-ocean circulation. Nature 342, 637–642.

Fairbanks, R.G., Mortlock, R.A., Chiu, T.-C.h., Cao, L., Kaplan, A., Guilderson, T.P., Fairbanks, T.W., Bloom, A.L., Grootes, P.M., Nadeau, M.J., 2005. Radiocarbon calibration curve spanning 0 to 50,000 years BP based on paired 230Th/234U/238U and 14C dates on pristine corals. Quaternary Science Reviews 24, 1781–1796.

Hald, M., Steinsund, P.I., Dokken, T., Korsun, S., Polyak, L., Aspeli, R., 1994. Recent and Late Quaternary distribution of *Elphidium excavatum* f. *clavatum* in the Arctic seas. Cushman Foundation Special Publication 32, 141–153.

Hald, M., Kolstad, V., Polyak, L., Forman, S.L., Herlihy, F.A., Ivanov, G., Nescheretov, A., 1999. Late-glacial and Holocene paleoceanography and sedimentary environments in the St. Anna Trough, Eurasian Arctic Ocean margin. Palaeogeography, Palaeoclimatology, Palaeoecology 146, 229–249.

Hald, M., Dokken, T., Mikalsen, G., 2001. Abrupt climatic change during the last interglacial – glacial cycle in the polar North Atlantic. Marine Geology 176, 121–137.

Hald, M., Husum, K., Vorren, T.O., Grøsfeld, K., Jensen, H.B., Sharapova, A., 2003. Holocene climate in the subarctic fjord Malangen, northern Norway: a multi-proxy study. Boreas 32, 543–559.

Hald, M., Ebbesen, H., Forwick, M., Gothliebsen, F., Khomenko, L., Korsun, S., Olsen, L.R., Vorren, T.O., 2004. Holocene paleoceanography and glacial history of the West Spitsbergen area, Euro-Arctic margin. Quaternary Science Reviews 23, 2075–2088.

Hald, M., Andersson, C., Ebbesen, H., Jansen, E., Klitgaard-Kristensen, D., Risebrobakken, B., Salomonses, G.R., Sarnthein, M., Sejrup, H.P., Telford, R.J., 2007. Variations in temperature and extent of Atlantic Water in the northern North Atlantic during the Holocene. Quaternary Science Reviews 26, 3423–3440.

Hammer, Ø., Harper, D.A.T., Ryan, P.D., 2001. PAST: Paleontological Statistics software package for education and data analysis. Palaeontologia Electronica 4 (1) (9 pp.).

Hubberten, H.W., Andreev, A., Astakhov, V.I., Demidov, I., Dowdeswell, J.A., Henriksen, M., Hjort, C., Houmark-Nielsen, M., Jakobsson, M., Kuzmina, S., Larsen, E., Lunkka, J.P., Lyså, A., Mangerud, J., Möller, P., Saarnisto, M., Schirrmeister, L., Sher, A.V., Siegert, C., Siegert, M.J., Svendsen, J.I., 2004. The periglacial climate and environment in northern Eurasia during the Last Glaciation. Quaternary Science Reviews 23 (11–13), 1333–1357.

Ivanov, V.V., Golovin, P.N., 2007. Observations and modeling of dense water cascading from the northwestern Laptev Sea shelf. Journal of Geophysical Research 112, C09003. http://dx.doi.org/10.1029/2006JC003882, 2007.

Ivanova, E.V., Murdmaa, I.O., Duplessy, J.-C., Paterne, M., 2002. Late Weichselian to Holocene paleoenvironments in the Barents Sea. Global and Planetary Change 34, 209–218.

Jakobsson, M., Long, A., Ingólfsson, Ó., Kjær, K.H., Spielhagen, R.F., 2010. New insights on Arctic Quaternary climate variability from palaeo-records and numerical modeling. Quaternary Science Reviews 29, 3349–3358.

Karklin, V.P., Karelin, I.D., 2009. Seasonal and multiannual variability of the sea-ice regime in the Laptev and East Siberian seas. In: Kassens, H., Lisitzin, A.P., Thiede, J., Polyakova, Ye.I., Timokhov, L.A., Frolov, I.E. (Eds.), Sistema Morya Laptevykh i Prilegayushchikh Morei Arktiki: Sovremennoe Sostoyanie i Istoriya Razvitiya. (System of the Laptev Sea and the Adjacent Arctic Seas: Modern and Past Environments). Moscow Univ. Press, Moscow, pp. 187–201 (in Russian with English Abstr.).

Klyuvitkina, T.S., 2007. Paleogeography of the Laptev Sea during the late Pleistocene and Holocene inferred from fossil microalgae. PhD Thesis, Geographical Faculty, Moscow State University, Moscow (in Russian).

Klyuvitkina, T.S., Bauch, H.A., 2006. Hydrological changes in the Laptev Sea during the Holocene inferred from the studies of aquatic palynomorphs. Oceanology 46 (6), 859–868.

Klyuvitkina, T.S., Novichkova, Ye.A., Polyakova, Ye.I., Matthiessen, J., 2009. Aquatic palynomorphs in the Arctic seas sediments and their significance for late Pleistocene and Holocene paleoceanographic reconstructions (by the example of the White and Laptev seas). In: Kassens, H., Lisitzin, A.P., Thiede, J., Polyakova, Ye.I., Timokhov, L.A., Frolov, I.E. (Eds.), System of the Laptev Sea and the Adjacent Arctic Seas: Modern and Past Environments. Moscow University Press, Moscow, pp. 448–465 (in Russian with English abstract).

Knies, J., Vogt, C., Stein, R., 1999. Late Quaternary growth and decay of the Svalbard/Barents Sea ice sheet and paleoceanographic evolution in the adjacent Arctic Ocean. Geo-Marine Letters 18, 195–202.

Knies, J., Nowaczyk, N., Müller, C., Vogt, C., Stein, R., 2000. A multiproxy approach to reconstruct the environmental changes along the Eurasian continental margin over the last 150000 years. Marine Geology 163, 317–344.

Knudsen, K.L., Seidenkrantz, M.-S., 1994. *Stainforthia feylingi* new species from arctic to subarctic environments, previously recorded as *Stainforthia schreibersiana* (Czjzek). Cushman Foundation for Foraminiferal Research, Special Publication 32, 5–13.

Knudsen, K.L., Stabell, B., Seidenkrantz, M.-S., Eiriksson, J., Blake Jr., W., 2008. Deglacial and Holocene conditions in northernmost Baffin Bay: sediments, foraminifera, diatoms and stable isotopes. Boreas 37, 346–376.

Koç, N., Klitgaard-Kristensen, D., Hasle, K., Forsberg, C.F., Solheim, A., 2002. Late glacial palaeoceanography of Hinlopen Strait, northern Svalbard. Polar Research 21 (2), 307–314.

Korsun, S.A., Pogodina, I.A., Tarasov, G.A., Matishov, G.G., 1994. Foraminifera of the Barents Sea (Hydrobiology and Quaternary paleoecology). Kola Scientific Centre RAS, Murmansk Marine Biological Institute, Apatity. (in Russian).

Kristoffersen, Y., Coakley, B., Jokat, W., Edwards, M., Brekke, H., Gjengedal, J., 2004. Seabed erosion on the Lomonosov Ridge, central Arctic Ocean: a tale of deep draft icebergs in the Eurasia Basin and the influence of Atlantic water inflow on iceberg motion? Paleoceanography 19, PA3006. http://dx.doi.org/10.1029/2003PA000985.

Lubinski, D.J., Polyak, L., Forman, S.L., 2001. Freshwater and Atlantic water inflows to the deep northern Barents and Kara seas since ca 13 ^{14}C ka: foraminifera and stable isotope. Quaternary Science Reviews 20, 1851–1879.

Matthiessen, J., de Vernal, A., Head, M., Okolodkov, Yu., Zonneveld, K., Harland, R., 2005. Modern organic-walled dinoflagellate cysts in Arctic marine environments and their (paleo-) environmental significance. Paläontologische Zeitschrift 79 (1), 3–51.

Mudie, P.J., 1992. Circum Arctic Quaternary and Neogene marine palynofloras: paleoecology and statistical analysis. In: Head, M.J., Wrenn, J.H. (Eds.), Neogene and Quaternary Dinoflagellate Cysts and Acritarchs. American Association of Stratigraphic Palynologists Foundation, Dallas, pp. 347–390.

Mudie, P.J., Rochon, A., 2001. Distribution of dinoflagellate cysts in the Canadian Arctic marine region. Journal of Quaternary Science 16 (7), 603–620.

Mueller-Lupp, T., Bauch, H.A., Erlenkeuser, H., Hefter, J., Kassens, H., Thiede, J., 2000. Changes in the deposition of terrestrial organic matter on the Laptev Sea shelf during the Holocene: evidence from stable carbon isotopes. International Journal of Earth Sciences 89, 563–568.

Murdmaa, I., Polyak, L., Ivanova, E., Khromova, N., 2004. Paleoenvironments in Russkaya Gavan' Fjord (NW Novaya Zemlya, Barents Sea) during the last millennium. Palaeogeography, Palaeoclimatology, Palaeoecology 209, 141–154.

Naidina, O.D., Bauch, H.A., 2011. Early to middle Holocene pollen record from the Laptev Sea (Arctic Siberia). Quaternary International 229 (1–2), 84–88.

Nørgaard-Pedersen, N., Spielhagen, R.F., Erlenkeuser, H., Grootes, P.M., Heinemeier, J., Knies, J., 2003. Arctic Ocean during the Last Glacial Maximum: Atlantic and polar domains of surface water mass distribution and ice cover. Paleoceanography 18 (3), 1063. http://dx.doi.org/10.1029/2002PA000781.

Osterman, L.E., Poore, R.Z., Foley, K.M., 1999. Distribution of benthic foraminifers (>125 μm) in the surface sediments of the Arctic Ocean. USGS Bulletin, 2164.

Polyak, L., Mikhailov, V., 1996. Post-glacial environments of the southeastern Barents Sea: foraminiferal evidence. In: Andrews, J.T., Austin, W.E.N., Bergsten, H., Jennings, A.E. (Eds.), Late Quaternary Palaeoceanography of the North Atlantic Margins: Geol. Soc. Spec. Publ., 111, pp. 323–337.

Polyak, L., Forman, S.L., Herlihy, F.A., Ivanov, G., Krinitsky, P., 1997. Late Weichselian deglacial history of the Svyataya (Saint) Anna Trough, northern Kara Sea, Arctic Russia. Marine Geology 143, 169–188.

Polyak, L., Korsun, S., Febo, L., Stanovoy, V., Khusid, T., Hald, M., Paulsen, B.E., Lubinski, D.A., 2002. Benthic foraminiferal assemblages from the southern Kara Sea, a river-influenced arctic marine environment. Journal of Foraminiferal Research 32 (3), 252–273.

Polyak, L., Darby, D.A., Bischof, J.F., Jakobsson, M., 2007. Stratigraphic constraints on late Pleistocene glacial erosion and deglaciation of the Chukchi margin, Arctic Ocean. Quaternary Research 67, 234–245.

Polyak, L., Alley, R., Andrews, J.T., Brigham-Grette, J., Cronin, T., Darby, D., Dyke, A.S., Fitzpatrick, J.J., Funder, S., Holland, M., Jennings, A.E., Miller, G.H., O'Regan, M., Savelle, J., Serreze, M., St.John, K., White, J.W.C., Wolff, E., 2010. History of sea ice in the Arctic. Quaternary Science Reviews 29 (15–16), 1757–1778.

Polyakov, I.V., Beszczynska, A., Carmack, E.C., Dmitrenko, I.A., Fahrbach, E., Frolov, I.E., Gerdes, R., Hansen, E., Holfort, J., Ivanov, V.V., Johnson, M.A., Karcher, M., Kauker, F., Morison, J., Orvik, K.A., Schauer, U., Simmons, H.L., Skagseth, Ø., Sokolov, V.T., Steele, M., Timokhov, L.A., Walsh, D., Walsh, J.E., 2005. One more step toward a warmer Arctic. Geophysical Research Letters 32, L17605. http://dx.doi.org/10.1029/2005GL023740.

Rasmussen, T.L., Thomsen, E., Ślubowska, M.A., Jessen, S., Solheim, A., Koç, N., 2007. Paleoceanographic evolution of the SW Svalbard margin (76°N) since 20,000 ^{14}C yr BP. Quaternary Research 67, 100–114.

Reimnitz, E., Kempema, E.W., Barnes, P.W., 1987. Anchor ice, seabed freezing, and sediment dynamics in shallow Arctic seas. Journal of Geophysical Research 92 (C13), 14,671–14,678.

Reimnitz, E., Dethleff, D., Nürnberg, D., 1994. Contrasts in Arctic shelf sea-ice regimes and some implications: Beaufort Sea versus Laptev Sea. Marine Geology 119, 215–225.

Renssen, H., Seppä, H., Heiri, O., Roche, D.M., Goosse, H., Fichefet, T., 2009. The spatial and temporal complexity of the Holocene thermal maximum. Nature Geoscience 2, 411–414. http://dx.doi.org/10.1038/NGEO513.

Risebrobakken, B., Jansen, E., Andersson, C., Mjelde, E., Hevrøy, K., 2003. A high-resolution study of Holocene paleoclimatic and paleoceanographic changes in the Nordic Seas. Paleoceanography 18 (1), 1017. http://dx.doi.org/10.1029/2002PA000764.

Risebrobakken, B., Moros, M., Ivanova, E.V., Chistyakova, N., Rosenberg, R., 2010. Climate and oceanographic variability in the SW Barents Sea during the Holocene. The Holocene 20 (4), 609–621.

Rochon, A., de Vernal, A., Turon, J.-L., Matthiessen, J., Head, M.J., 1999. Recent dinoflagellate cysts of the North Atlantic Ocean and adjacent seas in relation to sea-surface parameters. American Association of Stratigraphic Palynologists Contribution Series, 35. 146 pp.

Romankevich, E.A., Vetrov, A.A., 2001. Tsikl ugleroda v arkticheskikh moryakh Rossii (Carbon cycle in the Arctic seas of Russia). Nauka, Moscow. (in Russian).

Rudels, B., Jones, E.P., Schauer, U., Eriksson, P., 2004. Atlantic sources of the Arctic Ocean surface and halocline waters. Polar Research 23 (2), 181–208.

Saloranta, T.M., Haugan, P.M., 2004. Northward cooling and freshening of the warm core of the West Spitsbegen current. Polar Research 23 (1), 79–88.

Sarnthein, M., Van Kreveld, S., Erlenkeuser, H., Grootes, P.M., Kucera, M., Pflaumann, U., Schulz, M., 2003. Centennial-to-millennial-scale periodicities of Holocene climate and sediment injections off the western Barents shelf, 75°N. Boreas 32, 447–461.

Schauer, U., Fahrbach, E., Osterhus, S., Rohardt, G., 2004. Arctic warming through the Fram Strait: oceanic heat transport from 3 years of measurement. Journal of Geophysical Research 109, C06106. http://dx.doi.org/10.1029/2003JC001823.

Schell, T.M., Scott, D.B., Rochon, A., Blasco, S., 2008. Late Quaternary paleoceanography and paleo-sea ice conditions in the Mackenzie Trough and Canyon, Beaufort Sea. Canadian Journal of Earth Sciences 45, 1399–1415.

Serreze, M.C., Holland, M.M., Stroeve, J., 2007. Perspectives on the Arctic's shrinking sea ice cover. Science 315, 1533–1536.

Ślubowska, M.A., Koç, N., Rasmussen, T.L., Klitgaard-Kristensen, D., 2005. Changes in the flow of Atlantic water into the Arctic Ocean since the last deglaciation: evidence from the northern Svalbard continental margin, 80°N. Paleoceanography 20, PA4014.

Ślubowska-Woldengen, M., Rasmussen, T.L., Koç, N., Klitgaard-Kristensen, D., Nilsen, F., Solheim, A., 2007. Advection of Atlantic Water to the western and northern Svalbard shelf since 17,500 cal yr BP. Quaternary Science Reviews 26, 463–478.

Ślubowska-Woldengen, M., Koç, N., Rasmussen, T.L., Klitgaard-Kristensen, D., Hald, M., Jennings, A.E., 2008. Time-slice reconstructions of ocean circulation changes at the continental margins of the Nordic and Barents Seas during the last 16,000 cal yr B.P. Quaternary Science Reviews 27, 1476–1492.

Spielhagen, R.F., Baumann, K.-H., Erlenkeuser, H., Nowaczyk, N.R., Nørgaard-Pedersen, N., Vogt, C., Weiel, D., 2004. Arctic Ocean deep-sea record of northern Eurasian ice sheet history. Quaternary Science Reviews 23, 1455–1483.

Spielhagen, R.F., Erlenkeuser, H., Siegert, C., 2005. History of freshwater runoff across the Laptev Sea (Arctic) during the Last deglaciaion. Global and Planetary Change 48 (1–3), 187–207.

Spielhagen, R.F., Werner, K., Aagaard Sørensen, S.A., Zamelczyk, K., Kandiano, E., Budeus, G., Husum, K., Marchitto, T.M., Hald, M., 2011. Enhanced modern heat transfer to the Arctic by warm Atlantic water. Science 331, 450–453.

Steffensen, J.P., Andersen, K.K., Bigler, M., Clausen, H.B., Dahl-Jensen, D., Fischer, H., Goto-Azuma, K., Hansson, M., Johnsen, S.J., Jouzel, J., Masson-Delmotte, V., Popp, T., Rasmussen, S.O., Rothlisberger, R., Ruth, U., Stauffer, B., Siggaard-Andersen, M.-L., Sveinbjornsdottir, A.E., Svensson, A., White, J.W.C., 2008. High-resolution Greenland ice core data show abrupt climate change happens in few years. Science 321, 680–684.

Stein, R., 2008. Arctic Ocean Sediments: Processes, Proxies, and Paleoenvironment. Elsevier, Amsterdam.

Stein, R., Fahl, K., 2000. Holocene accumulation of organic carbon at the Laptev Sea continental margin (Arctic Ocean): sources, pathways, and sinks. Geo-Marine Letters 20, 27–36.

Steinsund, P.I., Hald, M., 1994. Recent calcium carbonate dissolution in the Barents Sea: paleoceanographic implications. Marine Geology 117 (1–4), 303–306.

Steinsund, P.I., Polyak, L., Hald, M., Mikhailov, V., Korsun, S., 1994. Benthic foraminifera in surface sediments of the Barents and Kara seas. In: Steinsund, P.I., Benthic Foraminifera in surface sediments of the Barents and Kara seas: Modern and Late Quaternary applications. Ph.D. Thesis, Univ. of Tromsø, Norway, 61–102.

Stepanova, A.Yu., 2006. Late Pleistocene–Holocene and Recent Ostracoda of the Laptev Sea and their importance for paleoenvironmental reconstructions. Monograph Supplementary Issue of Russian Paleontological Journal 40 (2), 91–204.

Stepanova, A., Taldenkova, E., Bauch, H.A., 2003. Recent Ostracoda of the Laptev Sea (Arctic Siberia): taxonomic composition and some environmental implications. Marine Micropaleontology 48 (1–2), 23–48.

Stepanova, A., Taldenkova, E., Bauch, H.A., 2004. Ostracod species of the genus *Cytheropteron* from Late Pleistocene, Holocene and Recent sediments of the Laptev Sea (Arctic Siberia). Revista Española de Micropaleontología 36 (1), 83–108.

Stepanova, A., Taldenkova, E., Simstich, J., Bauch, H.A., 2007. Comparison study of the modern ostracod associations in the Kara and Laptev seas: ecological aspects. Marine Micropaleontology 63, 111–142.

Stepanova, A., Taldenkova, E., Bauch, H.A., in press. Ostracod paleoecology and environmental change in the Laptev and Kara seas (Siberian Arctic) during the last 18,000 years. Boreas. http://dx.doi.org/10.1111/j.1502-3885.2012.00254.x.

Svendsen, J.I., Alexanderson, H., Astakhov, V.I., Demidov, I., Dowdeswell, J.A., Funder, S., Gataullin, V., Henriksen, M., Hjort, C., Houmark-Nielsen, M., Hubberten, H.W., Ingólfsson, Ó., Jakobsson, M., Kjær Larsen, E., Lokrants, H., Lunkka, J.P., Lyså, A., Mangerud, J., Matiouchkov, A., Murray, A., Möller, P., Niessen, F., Nikolskaya, O., Polyak, L., Saarnisto, M., Siegert, C., Siegert, M.J., Spielhagen, R.F., Stein, R., 2004. Late Quaternary ice sheet history of eastern Eurasia. Quaternary Science Reviews 23, 1229–1271.

Taldenkova, E., Bauch, H.A., Stepanova, A., Dem'yankov, S., Ovsepyan, A., 2005. Last postglacial environmental evolution of the Laptev Sea shelf as reflected in molluscan, ostracodal and foraminiferal faunas. Global and Planetary Change 48 (1–3), 223–251.

Taldenkova, E., Bauch, H.A., Stepanova, A., Strezh, A., Dem'yankov, S., Ovsepyan, Ya., 2008. Postglacial to Holocene benthic assemblages from the Laptev Sea: paleoenvironmental implications. Quaternary International 183, 40–60.

Taldenkova, E., Bauch, H.A., Gottschalk, J., Nikolaev, S., Rostovtseva, Yu., Pogodina, I., Ya, Ovsepyan, Kandiano, E., 2010. History of ice-rafting and water mass evolution at the northern Siberian continental margin (Laptev Sea) during Late Glacial and Holocene times. Quaternary Science Reviews 29 (27–28), 3919–3935.

Tarasov, P.E., Peyron, O., Guiot, J., Brewer, S., Volkova, V.S., Bezusko, L.G., Dorfeyuk, N.I., Kvavadze, E.V., Osipova, I.M., Panova, N.K., 1999. Last Glacial Maximum climate of the former Soviet Union and Mongolia reconstructed from pollen and plant microfossil data. Climate Dynamics 15, 227–240.

Vogt, C., Knies, J., Spielhagen, R.F., Stein, R., 2001. Detailed mineralogical evidence for two nearly identical glacial/deglacial cycles and Atlantic water advection to the Arctic Ocean during the last 90,000 years. Global and Planetary Change 31, 23–44.

Volkmann, R., 2000. Planktic foraminifer ecology and stable isotope geochemistry in the Arctic Ocean: implications from water column and sediment surface studies for quantitative reconstructions of oceanic parameters. Berichte zur Polarforschung 361.

Whatley, R.C., Masson, D.G., 1979. The Ostracod genus *Cytheropteron* from the Quaternary and recent of Great Britain. Revista Espanola de Micropaleontologia 11 (2), 223–277.
Whatley, R.C., Eynon, M., Moguilevsky, A., 1996. Recent Ostracoda of the Scoresby Sund fjord system, East Greenland. Revista Espanola de Micropaleontologia 28 (2), 5–23.
Whatley, R.C., Eynon, M., Moguilevsky, A., 1998. The depth distribution of Ostracoda from the Greenland Sea. Journal of Micropalaeontology 17, 15–32.
Wollenburg, J.E., Mackensen, A., 1998. On the vertical distribution of living (Rose Bengal stained) benthic foraminifers in the Arctic Ocean. Journal of Foraminiferal Research 28 (4), 268–285.
Wollenburg, J., Mackensen, A., 2009. The ecology and distribution of benthic foraminifers at the Håkon Mosby mud volcano (SW Barents Sea slope). Deep Sea Research Part I: Oceanographic Research Papers 56 (8), 1336–1370.
Wollenburg, J.E., Knies, J., Mackensen, A., 2004. High-resolution paleoproductivity fluctuations during the past 24 kyr as indicated by benthic foraminifera in the marginal Arctic Ocean. Palaeogeography, Palaeoclimatology, Palaeoecology 204, 209–238.